
Predicting the future location of lymph nodes in rectal cancer patient during treatment using scans acquired prior to treatment

Master thesis
22gr403

Aalborg University
Faculty of Health Science and Technology

© 22gr403, Aalborg University, spring 2022.

Attributions

This report was written in overleaf [L^AT_EX](#).

[Google Sheets](#) by [Google Inc.](#), licensed as [Open Source](#), was used.

Online meetings held with [Microsoft Teams](#) by [Microsoft](#) licensed under [Microsoft 365 Apps for enterprise](#).

For programming [Anaconda](#) by [Anaconda Inc](#) which was licensed under [3-clause BSD License](#)

IDE used for programming is [PyCharm](#) by [JetBrains s.r.o.](#) which is licensed under [Free education license](#)

Computing and training of the network models, was performed using [Claudia](#) provided by [Aalborg University](#)



AALBORG UNIVERSITY
STUDENT REPORT

Department of Health Science and Technology

Fredrik Bajers Vej 7

DK-9220 Aalborg Ø

<https://www.hst.aau.dk/>

Title:

Predicting the future location of lymph nodes in rectal cancer patient during treatment using scans acquired prior to treatment

Theme:

Biomedical image analysis and processing

Project period:

Spring 2022

Project group:

22gr403

Participants:

Anne Haahr Andresen

Supervisor:

Lasse Riis Østergaard, MSc, PhD

External collaborators:

Dennis Tideman Arp, MSc, PhD student

Laurids Østergaard Poulsen, MD, PhD

Martin Skovmos Nielsen, MSc, PhD

Copies:

Pages: 63

Date of completion:

June 1, 2022

ii

Abstract:

Rektum kræft er blandt de hyppigst forekommende, typer af kræft, og det har en dødelighed på mere en 900,000 af 2020. Til behandlingen af rektum kræft tilbydes der på nuværende tidspunkt tre behandlingsformer, operation, kemoterapi og stråleterapi, som oftest tilbydes i kombination. Der er dog i de senere år sket et skift i behandlingsstrategien, hvorledes at der anvendes kemoterapi og radioterapi som behandlingsmetode uden operation. Denne tilgang til behandling har vist sig effektiv dog, er det ikke alle patienter der bliver kureret eller respondere på behandlingen. Derfor er det foreslået at øge stråle dosis, hvilket har øget antallet af patienter der responderer på behandlingen. Dog medfølger der med den øgede stråle dosis en række bivirkninger, som følge af skade på rask væv og derfor skal området der bestråles. Dette område skal dog under hele behandlingen dække det kræft ramte væv og derfor skal der tages højde for bevægeligheder der forekommer. Derfor er det foreslået at indsnævre området ved hjælp af bevægeligheden. Dog optages der normalt ikke skanninger under behandlingsforløbet og derfor er placering a kræft vævet ikke kendt. Derfor er der foreslået et design til en algoritme, bestående af et regressions neuralt netværk, til at prædiktere den fremtidige position af lymfeknuder. Dette er gjort med udgangspunkt i en række prædiktors der er udvalgt af udtrækket ud udgangspunkt i litteraturen. Resultaterne for the implementerede model viser en stabil træning, dog opnås der en relativ høj MSE, og dermed er yderligere udvikling a modellen eller udviklingen af en ny model nødvendigt for at opnå en model med højere prædiktions nøjagtighed.

Preface

This master thesis was made by group 22gr403 with the theme of biomedical signal and image processing at Aalborg university. This was based on a cooperation with department of medical physics at the department of oncology at Aalborg university hospital, which provided data and knowledge to the project.

The author would like to thank Lasse Riis Østergaard, PhD, associator professor at Aalborg univeristy for the continued collaboration and supervision provided through the last year an a half. Furthermore, the author would like to thank Dennis Tideman Arp, PhD-student, Laurids Østergaard Poulsen, MD, PhD and Martin Skovmos Nielsen, PhD from department of medical physics and department of oncology at oncology for the contributions to the master thesis.

Aalborg University, May 31, 2022.

Anne Haahr Andresen
aandr17@student.aau.dk

Reading Guide

For the current project employs the Harvard citation style for referencing of sources, as the the last name of the main author is presented followed by the year of publication. These are presented in two ways, as either an active or passive citation. Active citation is used when the source is placed within the sentence as part of the statement and is not surrounded by parenthesis. The passive citation is employed when the source is used following the sentence at the end of a sentence, and is indicated by a source enclosed by parenthesis.

The bibliography on page on [page 65](#) is structured in alphabetic order in accordance with the last name of the main author. If the author is not available, the article is listed according to the first word of the title. For the figures presented in the rapport, figures with citations is from other works. However if no citation is by the figures these are made by the author or from the provided dataset.

Citation Style

An example of the citations is presented here:

Passive citation: [R. Siegel, DeSantis, and Jemal 2014]

Active citation: R. Siegel, DeSantis, and Jemal 2014

Contents

1	Summary	1
2	Resume	3
3	Introduction	5
4	Background	7
5	Research question	19
6	Data	21
7	Methods	23
8	Results	43
9	Discussion	53
10	Conclusion	59
11	Portfolio	61
	Bibliography	65
	Appendix A Literature search	69

This page intentionally left blank.

1 Summary

Rectum cancer is one of the most common types of cancer, which has a mortality of more than 900,000 as of 2020. Current treatment consist of chemotherapy, surgery and radiotherapy, which are often combined for treatment of rectum cancer. However in recent years there has been a shift in the treatment strategy where surgery is omitted. This shift is occurring as a fraction of the patients receiving chemo-and radiotherapy obtained a curative stage, without surgery and therefore surgery was omitted. There is a remaining patient population which did not obtain a curative stage or did not respond to the treatment and therefore it was suggested to increase the dosage of radiotherapy. This increase the rate of patients which benefited from this treatment approach, but it likewise produced a new set of side effects as more damaged was imposed on the healthy tissues which received the higher dosages. Therefore to omit these side effects it has been suggested to reduce the area in which this is applied. As there is motility within the area, it has been suggested that it is performed by quantifying these motilities and based on these reduce the area, to retain coverage of the cancer tissue. This requires knowledge of the current of stage of the pelvis during treatment which is not available as scans usually are acquired prior to treatment. Therefore this new locations has to be predicted. For this purpose different models has been proposed to predict a subsequent position of an organ. However, none of these are for the lymph nodes and therefore the aim of the project was to develop a model which could predict the future location of these during treatment.

The pipeline developed for this purpose consisted of initial identification and quantification of predictors which could be indicative of the future location or motility. Subsequent to this data augmentation was performed as a deep learning model requires a large dataset. Data augmentation was performed using a stacked autoencoder to increase the size of the dataset. For prediction of a future lymph node location during treatment a combination of previously proposed models was utilized. This consisted of deep learning and regression models which combined produced a deep learning regression model. The structure design was based on the aim, the output of the predictors and the target values. This produces a network with three branches which produced two separate models which predicted three outputs representing the location of a lymph node.

Validation on the predictors and the prediction model found that there was an indication that the assumptions made for the identified predictors was true, both in a qualitative and quantitative assessment. As associations between the predictors was found, different models were trained of different versions of the dataset where it was found that the model which obtained the lowest loss was the model trained on the full dataset and therefore the final validation was performed on the model. The final validation of the model obtained a high mean square error for all three outputs, and therefore further

development of a model is needed to obtain a high accuracy for the determination of the lymph node location

2 Resume

Rektum kræft er en af de hyppigste forekommende kræfttyper med mere end 900.000 dødsfald. Den nuværende behandlingsform består af kemoterapi, operation og radioterapi, hvilket som udgangspunkt tilbydes samlet. Der er dog ved at ske et skift i behandlingsstrategi, hvorledes at man udgår at anvende operation som en behandling og udelukkende anvender kemo-og radioterapi, hvorledes en del af patientgruppen opnår at bliver kræft fri. Det er dog ikke alle der bliver kræft fri eller respondere på behandlingen og derfor er det foreslået at øge dosis af radioterapien til at forbedre raten af patienter der responderer. Dette forbedrede responsraten, men medførte en række nye bivirkninger som er et resultat af skade på det sundævæv der ligeledes bliver ramt af den højere stråledosis. Derfor er det foreslået at indsnævre området for radioterapien påføres. Dette skal dog gøres således at kræftvævet stadig får påført radioterapi og derfor er det foreslået at reduktionen af områder gøres på baggrund af bevægeligheden af vævet. Der optages dog ingen skanninger under behandling og derfor skal placeringen af vævet prædikeres. På nuværende tidspunkt er der udviklet forskellige metoder for prædiktionen af dette, dog er ingen af disse udviklet til lymfeknuder og derfor er formålet med projektet at undersøge om der kunne udvikles en metode dette.

Til dette er der udviklet en pipeline der indledningsvis bestod i at identificere og kvantificere forskellige prædiktors der kunne være indikative for bevægeligheden eller der fremtidige placering af lymfeknuderne. Dette er efterfulgt af en dataaugmentation idet der anvendes en deep learning model, hvilket typisk kræver en større mængde data. Denne augmentation udføres ved brug af en stacked autoencoder til at udvide datasættet. Prædiktionsmodellen består af en deep learning regression model som er inspireret af tidligere udviklede modeller. Selve strukturen for denne model er designet med baggrund i målet for modellen, outputtet af prædiktorerne og output placeringerne der skulle prædikeres. Dette producerede to modeller der samlet prædikterede værdier der repræsenterede lymfeknude placeringen.

Resultaterne for prædiktorerne af prædiktionsmodellen fandt and der var en indikation på at de antagelser for associationerne der blev anvendt i forbindelse med at udvælgelsen af prædiktors kunne være sand idet disse kom til udtryk både i den kvalitative og kvantitative evaluering. Fordi der ligeledes blev identificeres associationer mellem de forskellige prædiktors, blev flere modeller trænet på forskellige dataset, hvorledes det på baggrund af de forskellige træninger fremstod at den model der opnåede det lavest loss var den model der var trænet på det fulde dataset. Derfor var den endelige evaluering af prædiktionsmodellen. Den endelig model havde en høj MSE for alle tre outputs og derfor er der behov for yderligere udvikling af modellen eller udvikling af en ny model for at kunne opnå en model der med høj nøjagtighed kan prædiktere lymfeknude placeringen.

This page intentionally left blank.

3 Introduction

Rectal cancer is a deadly disease which has a mortality rate of 900,000 patients worldwide as of 2020. It is a disease in which cancerous tissue develops, accumulate and spread to the surrounding tissues and lymph nodes[R. L. Siegel et al. 2020] The conventional approach for treatment of this type of cancer consist of chemotherapy, surgery and radiotherapy, which is given as either a monotherapy or a consolidation of these. Currently a shift in treatment strategy is occurring as studies has shown that the surgical approach can be omitted for a portion of the patient population. This new approach referred to as *watch and wait* approach, uses a combination of radiotherapy and chemotherapy to obtain a curative stage for the patients. Watch and wait has shown promising results in regards to providing treatment to patients with rectal cancer, however a remaining patients group do not respond to this treatment, and therefore an increase the dosage of the radiotherapy treatment has been used. The increases in radiotherapy improved the response rate for the patients, but likewise produced new side effects. To avert these it has been proposed to reduce the area which this treatment is applied. The reduction of this area, requires knowledge regarding the location and motility of the tumor and lymph nodes to retain coverage of these. By quantifying and determining this, a reduction of the volume can be performed, which still contains the lymph nodes and tumor. However, as no scans are acquired during treatment the location during treatments has to be obtained by predicting the new position of the lymph nodes. This new location is the product of a displacement caused by varying organ stages which impacts the motility of others, and therefore these might also impact the lymph nodes and could therefore be used to determine the future position of lymph nodes. Therefore the initial research question is:

Which different factors could contribute to reducing the area of radiotherapy application to improve the treatment of rectum cancer?

This page intentionally left blank.

4 Background

4.1 Rectal cancer

Rectum cancer is a deadly disease which is associated with symptoms such as rectal bleeding, abdominal pain, tiredness, weakness and unexplained weight loss. [R. L. Siegel et al. 2020] This is because of development and accumulation of cancer cells within the rectum wall, which further migrates when malignant. These abnormal cells expands beyond the circumference of rectum wall and migrate to the surrounding tissues and enters the blood stream, and is transported to distant location where distant metastasis is then established. [Mahadevan 2014]

4.2 Treatment

The treatment of rectal cancer consists of three different approaches, chemotherapy, surgery and radiotherapy. The administration of these can be either as monotherapy or as a cumulation, where the recommendation suggests utilizing the cumulation of the treatment strategies for rectal cancer. [Poulsen,Laurids Østergaard and et. al 2021; Spindler,Karen-Lise Garm et.al 2021]

4.2.1 Surgery

Surgical intervention is a treatment which is rarely performed as a monotherapy but rather utilized in combination with radiotherapy and chemotherapy. During surgery the tumor, cancerous lymph nodes and the tissues surrounding these areas are likewise removed. Three different surgeries are used for the treatment of rectal cancer which are presented in the following list

- Open surgery
- Laparoscopic
- Transanal Endoscopic Microsurgery (TEM)

Regardless of the surgery approach it makes the patient more susceptible to infections, while other side effects is likewise affiliated with this treatment type. [Recio-Boiles et al. 2018; J. S. Wu 2007] The side effects are apparent as functional disturbances which includes irregular bladder function, impotency, retrograde ejaculation, and urinary retention that contributes to a reduced quality of life. [Dizdarevic et al. 2020; Recio-Boiles et al. 2018; J. S. Wu 2007]

4.2.2 Chemotherapy

The second treatment option is chemotherapy. This treatment is offered as either a monotherapy or in composite with radiotherapy, which is referred to as chemoradiotherapy (CRT). [Poulsen,Laurids Østergaard and et. al 2021] It is a treatment strategy which utilizes a drug with cytotoxic effects to induces cell death. Therefore, it is used to reduce the proliferation of cancer cells, and inhibit the tumor growth and metastasis. The cells death is induced by the drug which contains antineoplastic which interfere with the DNA of the cells, and then induce cell death. [*How does chemotherapy work?* [updated 22. august 2019] 2007]

4.2.3 Radiotherapy

Radiotherapy is the last treatment options of the currently recommended treatment strategy for rectal cancer. It is a treatment strategy which applies high energy x-rays to a local area containing cancerous tissue, to kill the cancer cells. The high energy x-rays alters the DNA, by creating an unstable environment where free radicals damage the DNA of the cells, and induces cell death. The area this is applied on is based on three volumes, which encloses different proportions of the cancerous tissue. The three volumes are the gross tumor volume, clinical target volume, and planning target volume. [Burnet et al. 2004]

Gross tumor volume

The smallest volume is the gross tumor volume. It is a volume which encloses the tumor and malignant lymph nodes and it is therefore anticipated to have the highest density of cancer cells. Therefore this could potentially be the recipient of higher dosages of radiotherapy. An example of the GTV is presented in figure 4.1. [E. V. Maani and C. V. Maani 2019; Burnet et al. 2004]



Figure 4.1: A representation of the GTV where the red delineation represents the GTV area that contains the tumor, while the brown delineation is the rectum.

Clinical target volume

The second volume defined for radiotherapy application is the clinical target volume (CTV). This volume encloses the GTV and is added to include the additional microscopic spread of the cancerous tissue surrounding the GTV. To achieve a curative stage this must be treated adequately as this margin encloses the local cancerous tissue. [E. V. Maani and C. V. Maani 2019; Burnet et al. 2004] A representation of the CTV is presented in figure 4.2.



Figure 4.2: A representation of the clinical target volume where the blue delineation represents the CTV, the red represents the tumor position and the brown represents the rectum.

Planning target volume

The planning target volume is the last volume which is added as a margin to manage the uncertainties in the beam positioning and ensure coverage of the cancerous tissue despite displacement of this. This margin encloses the CTV and therefore this volume contains healthy tissue. A representation of the PTV is presented in figure 4.3.



Figure 4.3: A representation of the planning target volumes extension which extends beyond the CTV in blue, and the GTV which is delineated in red. The PTV extension beyond the CTV is delineated in green.

4.3 Evolvement in rectal cancer treatment

Recently an evolvement in the treatment of rectal cancer has been occurring. This evolvement is based on a selective groups of rectal cancer patients which has obtained a curative stage without the utilization of surgical intervention. This watch and wait approach, has shown favoring results and it is estimated that upwards of 25 % of rectal cancer patients can obtain a curative stage with this treatment strategy. [Papaccio et al. 2020; Dossa et al. 2017] The watch and wait approach facilitates the avoidance of the side effects associated with the surgical intervention, mentioned in section 4.2.1, while also improving the conditions for organ preservation during treatment. [Papaccio et al. 2020]

4.3.1 Watch and wait

The watch and wait approach utilize chemo-radiotherapy (CRT) to obtain a curative stage, and thereby omits surgical intervention. [D'Amata et al. 2021; Bahadoer et al. 2022; Kim et al. 2021; Al-Najami et al. 2021; X. Zhang et al. 2022; Bahadoer et al. 2022] This has shown to be an effective treatment for a select portion of the patient group, as presented in table 4.1. A varying level of curative responses was achieved that ranged from 44 % in Al-Najami et al. 2021 to 84.3 % who obtained a curative stage in Shiao, Fakhoury, and J. Olsen 2020, which suggest that the watch and wait approach can be utilized for treatment and surgical approach can be omitted in select cases. The specification and results of the studies investigating this is presented in table 4.1.

Study	Year	n	Curative CRT
[Chadi et al.]	2017	608	68.4 %
[Kong et al.]	2017	256	69.2 %
[On, Shim and Aly et al.]	2019	248	84 %
[Shiao, Fakhoury and Olsen]	2020	306	84.3 %
[Al-Najami et al.]	2021	42	44 % – 76.4 %
[D'Amata et al.]	2021	55	75 %
[Kim et al.]	2021	19	68 %
[Bahadoes et al.]	2022	1552	74 % - 76%
[Zhang et al.]	2022	1254	74.8 %

Table 4.1: A representation of the number of patients (n) included in the studies and results of different which addresses the outcome of CRT treatment for the patients which initially had a positive response to CRT.

The results in table 4.1, are indicative of a positive response for the watch and wait approach. However, the results likewise show that not all patients responds to CRT and achieve a curative stage and there is likewise a patient group which do ot respond to CRT. These patient groups do not benefit from the watch and wait approach and therefore it has been suggested to increase the dosage of the radiotherapy, to improve the number of patients who benefits from this treatment and achieves a curative stage. [Hearn et al. 2021; Pang et al. 2021]

4.3.2 Increased radiotherapy dosage

As not all patients benefit or obtain a curative stage utilizing the traditional CRT treatment, it has been suggested to increase the dosage of radiotherapy to improve the response rate. A dosage increase can be obtained by increasing the dosage which is given at each treatment, or by giving the dosage corresponding to a regular treatment, but with additional treatments which accumulatively gives a higher dosage. [Rega et al. 2021] Independent of the approach for dosage increase, studies suggest an increased response rate for the patients receiving the higher dosages, when compared to patients receiving a dosage corresponding to current treatment. [Hearn et al. 2021; Pang et al. 2021] Specified response rates for the different studies is presented in 4.2.

Study	Year	n	CRT	Increased CRT
[Habr-Gama et al.]	2013	69	30 %	67 %
[São Julião et al.]	2018	221	27.4 %	33.4 %
[Habr-Gama et al.]	2019	81	58 %	78 %

Table 4.2: The results of comparative studies including n patients which have investigated higher dosages of radiotherapy, where the CRT represents the groups which has been recipient of normal radiotherapy and whom obtained a curative stage while the Extended CRT represent the groups which where recipient of a higher dosage of CRT who obtained a curative stage.

The higher dosages increased the response rate, so an improvement in the number of patients who benefits the higher dosage CRT treatment was achieved. With the higher response rate, there was likewise an improvement in the effectiveness of the treatment as there was an increased number of patients which responded to the CRT, and remained disease free which is indicative of improvement in disease free survival, when receiving higher dosages radiotherapy. [Lorimer et al. 2017] The rates for these results are presented in table 4.3.

Study	Year	n	pCR
[Huang, Lee, and Young]	2020	1186	66.1 %
[Hearn et al.]	2021	1817	24.1 %
[Delishaj et al.]	2021	TBD	28.2 %
[Wilson et al.]	2021	4359	35% – 40 %
[Fok et al.]	2021	127	43 % - 77.2 %

Table 4.3: The results of studies which have investigated higher dosages of radiotherapy, where the pCR represents the groups the recipient of a higher dosage of RT who obtained a pathological curative stage.

4.3.3 Side effects

Despite the improvements in the disease survival rate, the increased dosage of radiotherapy inflicted upon healthy tissues included in the PTV margin imposed damage. Therefore, this has been associated with new side effects which is present as a result of this newly damaged tissue. [Dizdarevic et al. 2020] The most commonly reported side effect is anorectal bleeding, which could be associated with tissue damage of the rectum. The higher dosages also caused inconsistent bowel and bladder movement, which could be because of the radiation damage inflicted on the bladder and bowel tissue, as these often lies within the PTV. [Mahadevan 2014; Dizdarevic et al. 2020]

4.4 Reduction of the planning target volume

Because of these side effects presented in section 4.3.3 it has been suggested to decrease the size of the PTV volume to reduce the exposure of healthy tissue, and lessen the damage. However, the PTV is introduced to address the displacement caused by motility to ensure coverage of the cancerous tissue, to administer adequate treatment. Therefore, the reduction of the PTV performed by quantification of the motility displacements, to obtain a new margin while ensuring the dosage delivery, has been suggested. [Björelund et al. 2018]

4.4.1 Motility of displacement estimation and relations

It is suggested to reduce the area of the application of the radiotherapy by quantifying the motility of the cancerous tissue and organs in the area. Motility is the motion of the organ which causes displacements of these in the pelvis. The causes of motility can be attributed to different factors which collectively produces a displacement. Organ deformation and size variations has been associated with the motility. In particular an association between the motility of the prostate and the size variation of the rectum and the bladder has been identified. [Pos et al. 2003; Bairstow et al. 2020; Roch, Zapatero, Castro, Hernández, et al. 2021] In addition this, the properties of the different tissues in

the pelvis, impacts the motility as different tissues have different elasticity, and thereby can expand and contract differently. [Rafaelsen et al. 2013] An depiction of different tissue types is presented in figure 4.4.

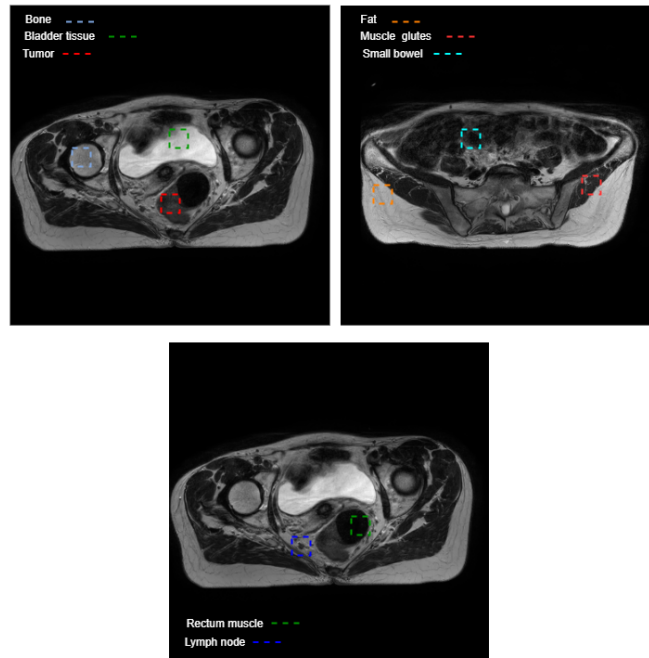


Figure 4.4: Illustration of the different tissue types in different layers of the pelvis

Quantification of this motility is a contributing factor which for reduction the PTV volume. To do this, different methods have been identified through the literature search presented in appendix A. These methods quantify the displacement caused by the motility. These can be divided into three subgroups, manual methods, semi-automatic methods, and automatic methods. Each of these sub-divisions consist of different methods which can be utilized to quantify the displacement of different organs.

Manual

Early methods to quantize the displacement of organs in the pelvic area is generally manually performed. These approaches manually annotate markers which represents either the center of mass (COM) or the delineation of the organ. Studies utilizing this is presented in table 4.4. Independently of the marker type, these are used as the starting point for the calculation where the displacement is quantified based on the difference between manually annotated markers and a reference markers. [Akino et al. 2013] This approach has been utilized by multiple studies on different imaging protocols. One protocol utilizes cine MRI to obtain the displacement margin based on largest distance between the COMs' by measuring the distance on acquired scans of the pelvic area,

between each of the frames. [Mah et al. 2002] A similar approach is employed for lymph node displacement, where the COM is likewise used as a measure, but with the reference COM being based on an average of the scans. [Akino et al. 2013] In addition to the cine imagery the same methodology has been used to determine the displacement between scans acquired before and after treatment to determine the displacement of the prostate between these scans. [Su et al. 2019; Bell et al. 2021]

Study	Year	Method	Displacement Organ	Reference
[Mah et al.]	2002	Fiducial marker	Rectum	Previous
[Akino et al.]	2013	Center fiducial	Lymph nodes	Previous
[Jensen et al.]	2019	Border fiducial marker	Cervix / Uterus	ITV(PTV)
[Su et al.]	2019	Center Fiducial marker	Lymph nodes	Prostate
[Bell et al.]	2021	Center Fiducial marker	Prostate	Previous

Table 4.4: The table contains an overview of article which utilize manual assessments to estimate the motility, of the organ, referred to as the displacement organ and the reference which is used as the starting point.

Semi-automatic

In addition to the manual methods which has been utilized to assess the displacement other methods which are less reliant on manual assessment than the previously presented methods has been developed. Those are semi-automatic approaches which although still reliant on interaction includes a automatic component, for the displacement quantification. Rather than obtaining the displacement as the direct distance between two points, these methods rely on defining the motility present, and based on this obtain the displacements. For this approach the methods presented in table 4.5 has been proposed. Collectively the methods utilize registration to determine this motility, where the type of registration is dependent on the purpose. Two registration types which are used in rigid registration and deformable image registration (DIR). Rigid registration performed by Pilskog et al. 2020 and Kershaw et al. 2018 is a registration which allows for translational and rotational deformation of scans to obtain the highest similarity between structures in the different scans, this is therefore be used to align anatomical structure such as bones and organ structures while retaining scaling difference that occurs between scans. The rigid registration is therefore used to to reduce the intra-patient movement, and then to quantify the displacement a DIR registration is performed subsequent to obtain an output which represents the displacement. [Kershaw et al. 2018; Pilskog et al. 2020] The deformable image registration is a registration method which uses translation, rotation and scaling of localized areas on the scans to calculate a deformation vector field (DVF) which represents the deformations. [Gonzalez, Woods, and Masters 2009] This is used to determine the motility of lymph nodes and vessels, by performing the registration on fiducial markers which have been implemented or annotated along the bony anatomy. The DVF then represents the translations, rotations, and scaling for the intra-patient

motion, when estimated for the bony anatomy, and the motility when performed in accordance with markers along the lymph nodes or vessels. [Kershaw et al. 2018; Pilskog et al. 2020; Marnouche et al. 2021]

Study	Year	Method	Displacement Organ
[Schippers et al.]	2014	Border annotation enclosure	Lymph nodes
[Groher et al.]	2017	Translations calculation/ Registration bony anatomy	Lymph nodes
[Kershaw et al.]	2018	Local rigid registration/ Distance	Lymph nodes
[Pilskog et al.]	2020	Rigid registration fiducial markers/ distance	lymph nodes
[Marnouche et al.]	2021	Registration border annotations/ distance	Vessels
[Krishnatry et al.]	2021	Registration bony anatomy/ Distance based on seeds	Lymph nodes

Table 4.5: This table is an overview of articles which utilize semi automatic assessments to calculate the motility, of the organs which is presented as the displacement organ

Automatic

Methods for quantification of the motility which not rely on manual intervention has been proposed in the recent years. These are methods which employ the registration component, which are equivalent to the presented registrations in section 4.4.1, but incorporate an additional component for quantification of the motility. Thereby a fully automatic quantification of displacement is performed, which is less prone to inter-observer variability, and all the margins are assess using the same methodology. Methods using rigid registration determine the displacements based on implanted fiducial markers which then provides the translation in three dimensions, which is extracted to represent the displacement. [Roch, Zapatero, Castro, Büchser, et al. 2019; Roch, Zapatero, Castro, Hernández, et al. 2021] Other methods uses DIR to provide a local images registration that produces a vector field to represent the displacements. These methods performed the DIR on implanted markers, annotated markers, or contours to calculate a vector field for the displacement of the markers, which translation is used as a pseudonym for the motion of the organ. Different placement of these markers is used to correct for intra-patient motion when placed along the bony anatomy, while markers placed along the organs provides the insight into the displacement of the organ. [Velema et al. 2012; Björelund et al. 2018; Pilskog et al. 2020; Marnouche et al. 2021; Lawes et al. 2021; Krishnatry et al. 2021] The output DVF of the DIR on markers along the organ, contains the vectors which length represents the displacement of the organ. The full overview of proposed automatic methods, and the organ which the displacement is quantified, is

presented in table 4.6.

Study	Year	Method	Displacement Organ
[Velema et al.]	2012	- Local deformable image registration - Calculate the vector lengths for 95 % describes shift.	Lymph nodes
[Björland et al.]	2018	Local deformable image registration between same image sections of different scans	Lymph nodes
[Roch , Zapatero et al.]	2021	3D rigid registration with fiducial markers	Rectum
[Lawes et al.]	2021	- Registration in relation to bones and prostate. - Registration in relation to bones and lymph nodes - Distance measurement based on fiducial markers for prostate, lymph nodes - Subtraction of prostate displacement from lymph node, to obtain lymph node motility	Lymph nodes

Table 4.6: This table is an overview of articles developed fully automatic methods to calculate the motility of an organ, represented in the table as the displacement organ

4.4.2 Current prediction models

There has been proposed a few models for prediction and description of the motility, however as few models has been proposed, the following section will not be constrained to the pelvis area.

The motility of organs in the rectum can be estimated, however, to do this scans was acquired prior to treatment, during treatment and post treatment or acquired but without treatment purpose. When administering radiotherapy treatment scans are acquired prior to treatment but not between treatment sessions therefore the displacement caused by motility during treatment cannot be directly assessed. The availability of the pre-treatment scans could be used to derive a model which can predict the future location or the displacement during treatment. Different models which can predict or associate the displacements has been presented and are presented in table 4.7. These, were identified through a structured literature search presented in appendix A, and are divided into two subgroups which consist of regression models and Markov models.

Regression models

Initially, models consisted of various regression models, where Qiu et al. 2007 and Van Liew et al. 2007 obtained a model for prediction of organ placement based on an input from surrogate marker on the skin. To do this a partial least regression models was trained, which produced a linear regression model. More recent studies likewise use regression models for prediction of the quantity of displacement, where Oates et al. 2017 used linear regression to associate MRI scans threshold with the probability of small prostate displacement and Chen et al. 2018 used a linear regression model to correlate internal and external markers to predict the internal motion of the tumor in the lungs.

GAN models

In addition to regression models two studies suggest using a Markov model or a Markov-like model based on a generative adversarial network (GAN) to predict subsequent location of an organ. The Markov model was based on cine MRI of the lungs and was used to predict the subsequent phase of the respiratory cycle given the previous image. A similar model was derived by Dai et al. 2021, where a GAN was used to extract features from two ultrasound images and used DIR to calculate a deformation vector field which was then used for prediction of the tumor location.

Study	Year	Model	Displacement Organ
[Qiu et al.]	2007	Partial least regression	Diaphragm
[Van Liew et al.]	2007	Partial least regression	Tumor
[Oates et al.]	2017	Regression model	Prostate
[Chen et al.]	2018	Regression model	Lungs
[A. Mirzapour et al.]	2018, 2019	Markov model - Semi markov model	Lungs
[Dai et al.]	2021	Markov-like network - GAN network	Tumor

Table 4.7: An overview of the identified articles which developed models for predicting the subsequent location of a particular organ or tumor.

This page intentionally left blank.

5 Research question

The patient group which has achieved the curative stage after CRT has facilitated a shift in the treatment strategy for rectal cancer, as this approach has shown to be an effective treatment strategy. However, a remaining group of patients do not obtain a curative stage or do not respond to the current CRT treatment, and it has therefore been suggested to increase the dosage of radiotherapy, which improved the rate of patients which responded to the treatment. This imposed new side effect and therefore to omit those a reduction in the area which the radiotherapy is applied, is proposed, to reduce the amount of healthy tissue which is damaged. [Björelund et al. 2018; Dizdarevic et al. 2020] However as scans are acquired prior to treatment and a coverage of the lymph nodes must remain to administer adequate treatment, the position of the lymph nodes during treatment has to be estimated. Current methods for predicting the future location of organs or tumors has been proposed and is presented in section 4.4.2. None of these are developed for the prediction of the pelvis lymph nodes locations. Therefore, developing a method for this, could contribute to reducing the area in the pelvis where the radiotherapy is applied, while ensuring coverage of the of the lymph nodes.

Research aim

How can a model for prediction of lymph node location be develop to predict the future placement of the lymph nodes in pelvis during treatment based on scans acquired prior to treatment

5.1 Objectives

To develop this methods sub goals are used to orient the process, throughout the development, and to achieve the different aspects of the projects and produce the final model. The objectives are therefore constructed to define different aspects which collectively defines a final model. The objectives collectively contribute to obtain a model which achieves the presented aim. In section 4.4.1 it was mentioned that different associations between the state of organs and tissue properties was associated with a higher motility and therefore these are used to define the state of the pelvis which further together with the treatment strategy can contribute to determine the current state and thereby the new placement of the lymph nodes. The objectives to obtain this is presented in the following list:

- Identify different factors which could affect the lymph node location
- Implement methods for quantification of the identified factors

- Develop a model which can predict the lymph node position during treatment
- Validate the prediction model performance quantitatively.

6 Data

6.1 Provided data

The data which is provided for the model construction is from the AMPERE study at Aalborg university hospital. Data consist of T2W 3 mm slices MRI, which were interpolated to obtain full 3D scans. 16 patients has been included, and for each patient a set of six scans are available, where three of the scans was acquired prior to treatment and three scans was acquired during treatment, an example of a scan, with annotations is presented in figure 6.1 Complimentary annotations for the scans vary, these available annotations and the scans. These are presented in the table 6.1.

Annotations	Patient
Bladder, bowel, CTV, Lymph node, Rectum	1, 2,3 ,4,5,6, 8, 9, 10
Bladder, bowel, CTV, lymph node, penile bulb, femoral heads, rectum, sacrum	7
Bladder, rectum, lymph node, tumor	11, 14, 15, 16
Lymph node, tumor	12, 13

Table 6.1: A representation of the annotations which is available for each patient, where tumor and lymph nodes is available for all patients while the remaining annotation differ

There is a different number of available number of scans for each patient, the number of scans available for each patient is presented in the following table 6.2

Patient	Number of scans
1,2,3,4,5,6,7,8,11,12,13, 14, 15, 16	6
9	5
10	4

Table 6.2: A table representing the number of scans that is available for each of the patients

6.2 Additional annotations

Additional annotations was acquired through last semester project which developed a model for detection of lymph nodes. As these annotations did not fully depict the lymph nodes, further development on this model has been performed, to obtain fuller outlines of the lymph nodes.



Figure 6.1: Illustration of a scan with complementary annotations

7 Methods

In the following section the methods for detection of lymph and tracking of these will be presented

7.1 Model pipeline



Figure 7.1: A representation of the pipeline which is designed to develop a model for prediction of lymph nodes future location. This consist of multiple steps which are illustrated by the individually colored boxes

The purpose of the project is to develop a model which can determine the location of lymph nodes for when a radiotherapy treatment is performed to give adequate treatment to these. The location of these vary though out the treatment course, because of the motility, size variations, and changes in disease progression, which is a results of one or more radiotherapy treatments given to the patient. However, as no scans are acquired during treatment the location of the lymph nodes has to be estimated based on scans acquired prior to treatment. Therefore, the following pipeline shown in figure 7.1 is proposed to determine the lymph node location in scans acquired prior to treatment. This pipeline presents a model, which based on pre-treatment scans should predict the future location of the lymph nodes in scans acquired during treatment. This prediction of the displacement is performed using different steps that collectively determines the lymph node position, in the during treatment scans. As input to the model different predictors which has been associated with the location of the lymph nodes or the motility, is used. The predictors which are introduced is influenced by different factors that affect the motility or location such as, the size, deformation of the surrounding organs, and the tissue properties which is presented in section 4.4.1, as these were associated with the motility or range of motion. Therefore these are introduced for prediction the lymph node location.

The model which is proposed for prediction of the future lymph node location is based on the previous studies which is presented in section 4.4.2 where recent model uses deep learning GAN, while earlier models use regression. By combining the deep learning model and regression models a deep learning regression model for prediction of the lymph node position is obtained. Deep learning regression model allows for identifying

and describe hidden patterns and associations, such as the ones found in Roch, Zapatero, Castro, Büchser, et al. [2019](#) and Mah et al. [2002](#), between the predictors to identify a specific target, such as location markers. Because a deep learning model is utilized, data augmentation is introduced as deep learning model requires a large amount of data for training, which the dataset, presented in chapter [6](#) do not provide. Therefore, to increase the size of the dataset, an approach recently adapted in biomedical classification problems and widely used in material science called stacked autoencoders is used for this purpose. [Wang, Liu, and Yuan [2020](#)]

7.2 Predictors

Different associations of the motility of organs in the pelvis region has been identified as mentioned in section 4.4.1 and 7.1. Therefore, to predict the lymph node location different factors, such as these association, which can contribute to determining the location during treatment are identified to be used as predictors. The predictors which has been identified are presented in figure 7.2 where size and tissue properties has been associated with a higher motility of an organs or tumor tissues in the pelvis, and therefore these are extracted and used as predictors, while the previous location is utilized to provide a distinguishment between the different lymph nodes while also providing an insight in to the area of the future location. [Dai et al. 2021; E. V. Maani and C. V. Maani 2019; Rafaelsen et al. 2013] The final predictor included is the motility as this provide an insight into the range of displacement.

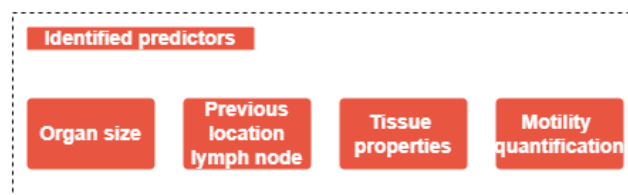


Figure 7.2: A representation of the different predictors which has been identified which could contribute to the prediction of the future position of the lymph nodes

The quantification of the presented predictors is achieved using different methods or measures which is presented in figure 7.3. These computes values which represents the specific predictors, and as there is different predictors there is likewise multiple methods which are used for the quantification of the individual predictors.

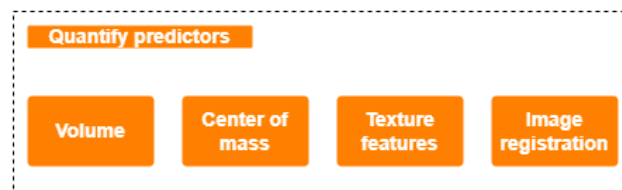


Figure 7.3: A representation of the the metrics or methods used to quantify the different predictors

Volume of bladder and rectum

The first predictor presented in figure 7.2 is the organ size, which is used as a predictor as the size of the particular organs, bladder and rectum was in Roch, Zapatero, Castro, Büchser, et al. 2019 and Mah et al. 2002 found to impact the motility of the prostate. In particular, these studies found that a larger diameter of the rectum and size of bladder was associated with a larger motility. The tumor volume is likewise included to describe the disease progression, as other factors describing this is unknown. The determination of the size is based on the 3-dimensional scans where the size of the organs is described with volume as a measure, as this quantifies an enclosed 3-dimensional space. [Adams and Essex 1999] This volume is based on the provided scans' annotations of the bladder, rectum and volume. Initially the voxel volume of one voxel is determined by calculating the product of the length of one voxel for the length, width and height. Once the voxel volume has been estimated the number of pixels which the organ consist is quantified, as the summation of voxel values > 0 which represents the number of voxels in the organ. The volume of the organ is then calculated as the obtained sum of voxels multiplied by the voxel volume for one voxel.

Lymph node location

The second predictor which is introduced in figure 7.2 for prediction of the location of lymph nodes is the location of the lymph nodes in the pre-treatment scans. There is multiple lymph nodes in the pelvis therefore to separate the lymph nodes while also determining the changes in position of equivalent lymph nodes, the previous locations for these used as a predictor.

As the lymph node position during treatment is predicted based on scans acquired prior to treatment, there is a progression in the size of the lymph nodes, which influence the location. Therefore, as a measure for the location, the center of mass (COM) used, as this is less affected by the size variations. The COM is the calculation of the 3-dimensional object relative to the mass distribution, so there is an equal distribution of mass surrounding the center. [Serway and Jewett 2018] The location of a lymph node given as the COM as this is less dependent of the size as the shrinkage and growth of the lymph node continues to progress before and during treatment, this continues to represent location independent of the increase in mass.

The calculation of center of mass for the lymph nodes is based on the annotated and the segmented lymph nodes from the previous project. On these segmentations and annotation the value of a voxel values > 0 represents mass. The center of the lymph nodes are then estimated by calculating the mean values of the mass for the height, width and length, as illustrated in equation 7.1. The mean values in each direction then collectively represents the center of mass, of the 3-dimensional lymph node.

$$Meanmass_x = \frac{M_x}{M_{Total}} \quad (7.1)$$

With multiple lymph nodes present in the pelvis, the COM is calculated within a constrained region therefore to calculate the true COM for the lymph nodes a coordinate defining the constrained region is added to calculate the true location on the full scan. The equation to calculate this is presented in 7.2.

$$\text{Truecenterofmass}_n = \frac{M_x}{M_{Total}} + x_n \quad (7.2)$$

In this equation the calculation of the true center of mass depends on the direction of the calculation where an x, y or z coordinate defining the area of the region is added to the direction which the mean of mass is calculated.

Tissue properties

Different lymph nodes are located in and adjacent to different types of tissues, as presented in figure 7.4. These tissue has different properties which could influence the motility as Rafaelsen et al. 2013 found a larger motility of the tumor placed in the perirectal fat when compared to the tumor in the rectum wall. Therefore, these different properties are included as a predictor 7.2. An approach to quantify these properties is to perform a texture analysis, which describes the appearances of a surface, such as a tissue, by calculating different representative values. To do this Haralich features are extracted, as these provides an insight into the appearance, feel, and consistency of the scan which collectively can describe the different properties of the tissue. [Löfstedt et al. 2019]



Figure 7.4: Illustration of the tissues, which the lymph nodes are located in and adjacent to. These mainly consist of fat and muscle tissue

To extract the Haralick features, a gray level co-occurrence matrix (GLCCM) is calculated, which is matrix that defines the distribution of co-occurring gray level voxels of the area surrounding the lymph node. Then based on this matrix different texture quantities is

extracted, which then describes the different characteristics of the tissues. [Miyamoto and Merryman 2005] An example of a representation of haralick features of fat tissue with and without lymph nodes is presented in figure 7.5.

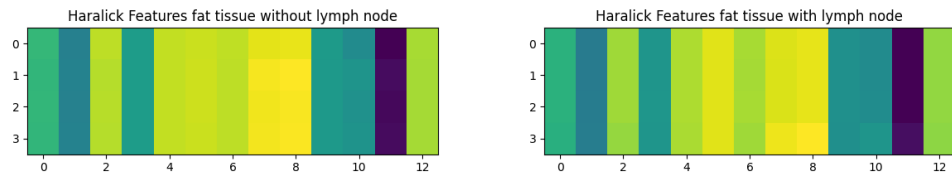


Figure 7.5: Representation of extracted haralick features from a tissue sample with and without a lymph node present in the tissue. Here an indexing of the different co-occurring intensity values, where a difference in tissue representation can be seen at the pixels labeled 5

Quantification of motion

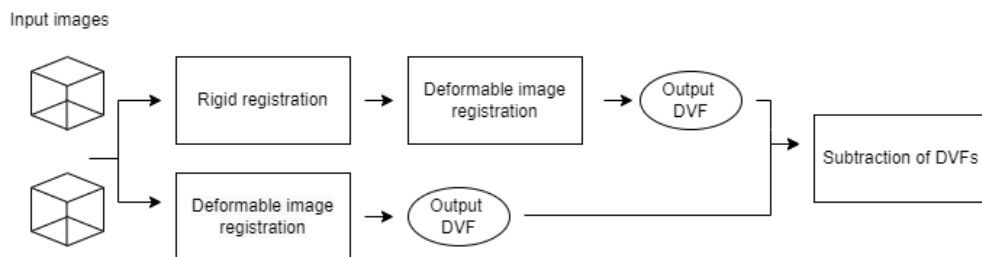


Figure 7.6: The implemented pipeline which used used to obtain the obtain the motility of the lymph nodes. Here the same two scans are registered in the first pipeline and in the second pipeline

The last predictor which is extracted for prediction of the future lymph node location is as presented in figure 7.2 the motility of the lymph nodes in the pre-treatment scans. This motility, is introduced as a predictor to indicate the range of motility and displacement for the lymph nodes.

The determination of this motility is based on a previous study Lawes et al. 2021 which uses image registration of the scans to quantify the motility. The motility is estimated

through two registration pipelines. The first pipeline is performed to determine the size variations, which consist of an initial rigid registration to create alignment of the structures in the scans, followed by a local DIR of the lymph nodes that produces a DVF which represents the size variations of the lymph nodes. A representation of the output DVF is illustrated in figure 7.8. The second pipeline consist a DIR, where the output DVF represent the motility and the size variations. The two DVFs from the registrations are subtracted to obtain the motility to obtain a vectors which represents the translation in the three dimensions which represent the medial-lateral (ML), anterior-posterior (AP) and the superior inferior (SI) translations. An example of the rigid registration is represented in figure 7.9.

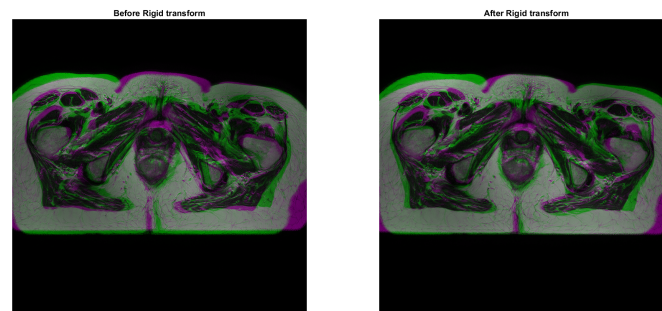


Figure 7.7: representation of images before and after registration, where alignments of the anatomical structure is presented as a shift can be seen of the green coloration of the edges of the tissue structure on the after image

For the rigid registration a translations and rotation of the scans is performed to obtain the highest correlation with the reference image. This translation and rotations are performed using transformation matrices for translation and rotation to deform the scans to obtain the highest similarity to the reference scan, which is the previous scan. [Hill et al. 2001] An example of this is represented in figure 7.7.

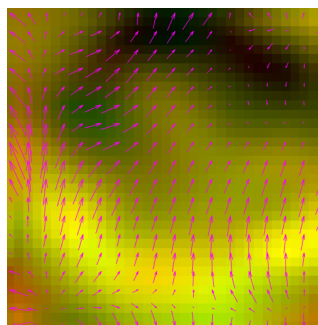


Figure 7.8: An illustration of the DVF after the initial registration pipeline which consisted of rigid registration followed by a DIR.

The DIR is based on the optical flow principle, which determines the motion of object, relative to the velocities of the intensities in the scans. Different tissue has varying intensity appearances as shown in figure 7.4 and therefor the determination of a shift in location can be based on those tissue representations. This is implemented as an optimization process which utilizes a similarity metric, normalized cross correlation, to determine the highest intensity similarity between the voxel and neighboring voxels of the next scan. The voxels with the highest similarity, within the neighborhood determines the shift, which is represented by a vector. This process is continuing and is performed for multiple neighborhoods of of voxels in the region containing the lymph nodes. The multiple calculated shift the generates a vector field which represents shift in location. [Lefébure and Cohen 2001; Brahme 2014] An illustration of an vector field representing the final shift for a lymph node is presented in figure 7.9.

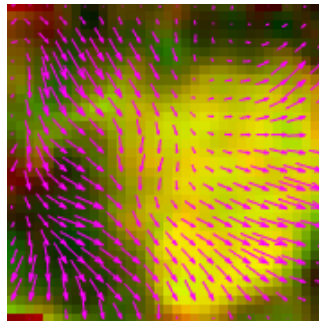


Figure 7.9: A representation of an up-scaled output vector field from the deformable image registration of a lymph node.

7.3 Data augmentation

Once the predictors has been extracted, the subsequent step is to augment the extracted data 7.10.



Figure 7.10: A representation of the current step in the full pipeline, with the method for the current step

As a deep learning model is proposed for the prediction of the lymph node location, data augmentation is needed. Deep learning models typically requires a large amount of data

when training, which is not available as presented in chapter 6. Therefore, to improve the training conditions for the model, the dataset is artificially increased using augmentation. A method for data augmentation approach which recently has been introduced approach to biomedical data for classification models and often used in material science is a stacked autoencoder, presented in figure 7.10. An autoencoder is a type of neural network which can be used to replicate the input data. It consist of two path an encoding path and a decoding path as illustrated in figure 7.11, where the encoding path compresses the data, and it dimensionalities, and the decoder reconstructs the data based on the compressed dataset. [Wang, Liu, and Yuan 2020]

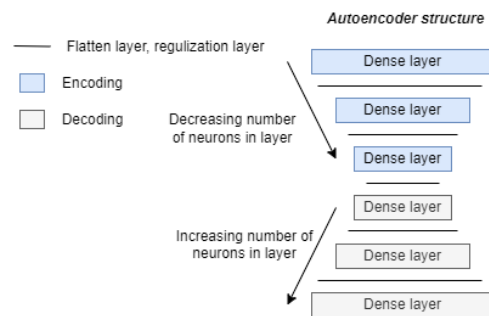


Figure 7.11: A representation an autoencoder structure, with the encoding an decoding path

The implemented autoencoder is trained to replicate the entire dataset, the extracted features, the future location of the lymph nodes, and after training the model from the autoencoder is used to predict on the same dataset. These predictions are then introduced into the dataset, to artificially increasing the dataset size. Subsequent to the first autoencoder a second auto encoder is trained on the new expanded dataset, and a prediction with the new model is then performed on the expanded dataset. These new predictions are then introduced to the dataset. The final number of autoencoders, is illustrated in figure 7.12.

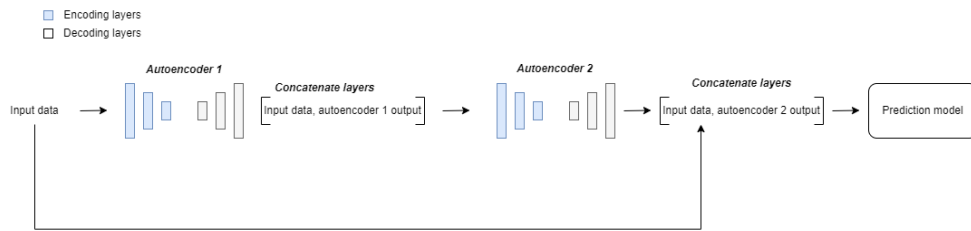


Figure 7.12: A representation of the stacked autoencoder principle, where autoencoder 2 is stacked on autoencoder 1, where the prediction of the autoencoder 1 is used as input for training autoencoder 2

7.4 Prediction model

Once the predictors has been extracted and augmented the subsequent step in the pipeline presented is to develop a prediction model. For this a deep learning regression model as presented in figure 7.13 is developed, to predict the future location of the lymph nodes.



Figure 7.13: The last step of the pipeline used for prediction of lymph node location

7.4.1 Deep learning regression model

Deep learning regression models is an approach that has emerged in the recent years which allows for identifying hidden patterns and associations which initially is not evident. Using artificial neurons, as shown in figure 7.14, arranged in layers deep learning regression models, identify these associations to create a model which can predict an output. [Ramsundar and Zadeh 2018]

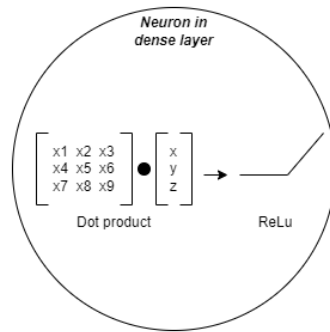


Figure 7.14: Artificial neuron in the dense layers, which computes the dot product which is then input the the activation function

When developing a deep learning model there is three main layers in which these neurons are arranged, input layers, hidden layers, and output layers, as illustrated in figure 7.15. The neurons in the hidden and output layers are computational units with two adjustable parameters the weight and bias, which are altered throughout training of the model. The weight parameter describes the importance of the different inputs to the neuron while the bias determines the offset for when the neuron is computationally active. The adjustment of these parameters is based on a loss function, which calculates the performance of the model, and through backpropagation using gradient descend alters weight and bias. [Ramsundar and Zadeh 2018]

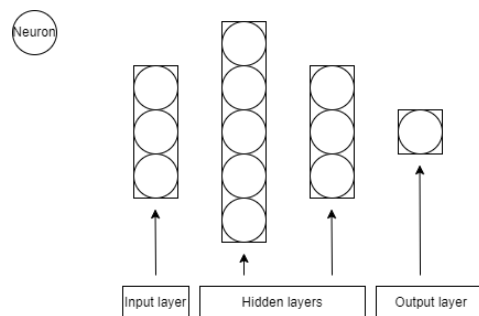


Figure 7.15: The basic layers in a neural network input layer, hidden layer and output layer.

Furthermore, non-adjustable parameters called hyperparameters are used to configure different aspects of the model training. These are pre-determined parameter, that are manually selected prior to training and impacts the networks performance and training. In different ways these contribute to defining the training of the model, and it can thereby impact the duration of training, the ability to learn, as well as how data is introduced to the network. The hyperparameter which determines how data is presented to the network is the batch size and epochs. These define the number of samples presented

to the network for each iteration, and the number of times in which the full dataset is presented to the network, during training. The duration of training, and the networks' ability to learn is affected by a hyperparameter called learning rate which determines the quantity of learning for each training iteration. [Ramsundar and Zadeh 2018]

7.4.2 Data splitting

To train and validate the model, the provided dataset has to be divided into subsets which individually contribute to improvement of the model. The dataset is divided into three sub-sets, which is used for the training of the model, validation of the model throughout training and test of the final model. [Ramsundar and Zadeh 2018; Hart, Stork, and Duda 2000] The full dataset is composed of the extracted features and the augmented features produced by the stacked autoencoders. Of the collective dataset approximately 66 % is augmented data points. For test-set 10 % of the full dataset is retained to the final evaluation of the model. The remaining dataset is split approximately 90% for training and 10% validation.

7.5 Implemented network

The design of the model for prediction is based on a multitude of factors, but with the backbone in the traditional structure for a prediction network. Each of these factors contribute with specifications to the network design, which is presented in this section. The initial layer of the network is the input layer, which is a distribution layer that is not computationally active, therefore the number of predictors determine the number of channels in the layer. The implemented input layer is a common layer feature distribution to the subsequent hidden layers in the network. The generalized construction of the hidden layers consist of dense layers, regularization layers L1, L2, and flatten layers, which each contribute with different computational functionalities to the network.

7.5.1 Layer types

Dense layer

A Dense layer is a commonly used layer which computes the output as the dot product of the input and the kernel summed with the bias and send through the loss function this principle is illustrated in figure 7.14. [Keras 2022]

L1 regularization

L1 regularization is to regularize the weights of the layer by shrinking these to zero. This thereby indirectly acts as a feature selector, as if the weight is zero, the particular input doesn't contribute to the collective output. [Tensorflow 2021] For this layer a particular

coefficient called lambda is used to determine the percentage of the weights which is to be returned to zero. Therefore a larger lambda value can return a high number of weights to zero, which can increase the loss. This is illustrated in figure 7.16. [*Tensorflow 2021*]

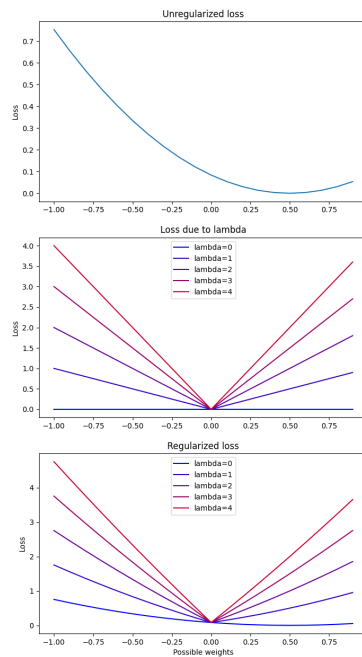


Figure 7.16: Illustration of L1 regularization with multiple lambda coefficient for regularization, in this particular case, a lambda value above zero return to many weight to zero and the loss increases.

L2 regularization

L2 regularization is likewise used in the initial layers as well as the final layers the regularization technique regularizes the weights evenly, by reducing the magnitudes of the weights evenly. This can therefore be used in layers which identify co-dependencies between features, to reduce overfitting. [Tensorflow 2021]

Similarly to L1 regularization a lambda coefficient is likewise used in L2 regularization. Here the term determines the penalty which is applied to the squared sum of the weights in the layer, this regularization is illustrated in figure 7.17. [Tensorflow 2021]

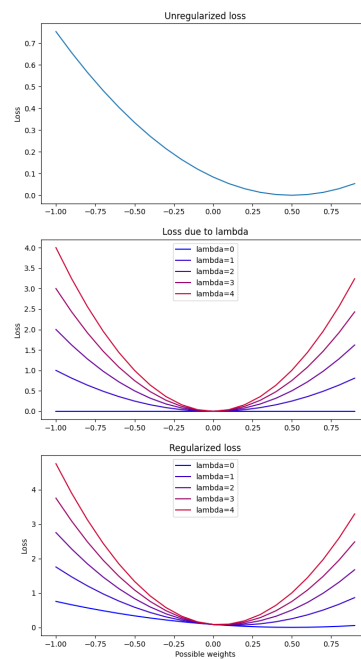


Figure 7.17: Illustration of L2 regularization with multiple lambda coefficient for regularization, a lambda value of above 0 increases the loss and thereby regularization is not need in the illustrated case.

Dropout layer

Dropout layer is introduced to reduce overfitting as well. This is performed by dropping part of the input data given to the subsequent layer. [Keras 2022]

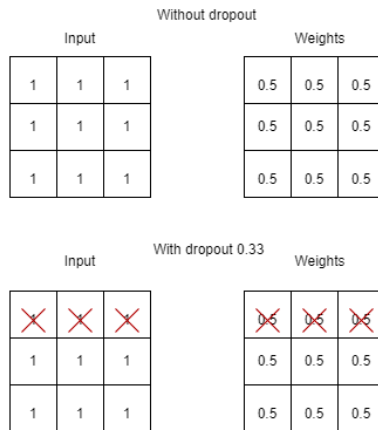


Figure 7.18: Illustration of functionality of the dropout layer

Flatten layer

The flatten layer is used for flattening the inputs to the next layer. So the output of the previous layer is reshaped into a 1D tensor which can then be passed to every subsequent neuron effectively. This improves effectiveness and reduce the likelihood of overfitting when dealing with multidimensional input data. [Keras 2022]



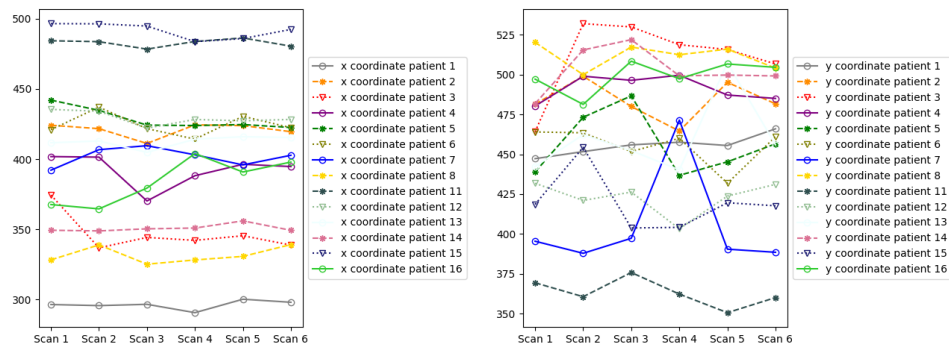
Figure 7.19: Illustration of the functionality of the implemented flatten layers

7.5.2 Structure of hidden layer and output layer

The layers which follow the input layers is the hidden layers which in the implemented structure consist of dense layers, regularization layers and a dropout layer. The arrangement of the layers following the input layer is impacted by the extracted predictors which produced a large range of values for the output targets, as there is a more diverse range

of y coordinates for location of the lymph nodes between scans for one patient when compared to the x and z direction as presented in figure 7.5.2. It can be difficult to predict such diverse output values on a small dataset, despite normalization of the inputs, and therefore the hidden layers following the input is two separate layers as presented in figure 7.21.

The hidden layers implement dense layer to identify the co-dependencies between the extracted predictors that was identified in previous studies presented in section 4.4.1. Moreover, other layer types are introduced to the hidden layers to stabilize the training conditions for the network, as few data samples are available. These layers are flatten layers, which reduce the dimensionalities of the data and regularization layers which evenly penalizes the weights in the neurons to prevent overfitting.



(a) Locations variation in the ML direction for a lymph nodes for the 14 patients across scans (b) Locations variation in the AP direction for a lymph nodes for the 14 patients across scans

Figure 7.20: A representation of the fluctuations of coordinate locations for lymph nodes where it can be see that a larger fluctuations and less systematic variation in the anterior posterior direction

Subsequent to the initial hidden layers, the network structure is refined to determine which of the predictors contribute to the prediction of the specific output target values, which describes the lymph node location. The target values consist of a 3-dimensional coordinate an x, y and z coordinate which represents the COM of the lymph nodes and therefore three output layers is implemented, which are connected to separate hidden layers. These hidden layer implements L1 regularization to prevent overfitting of the network during training while also contributing to refining the predictor selection for the individual the COM displacements in the ML, AP or SI direction. For the final hidden layer in the branches which predicts the lymph node position in the superior inferior direction, one dropout layer is included to further prevent overfitting. The final specified structure of layer is presented in figure 7.21.

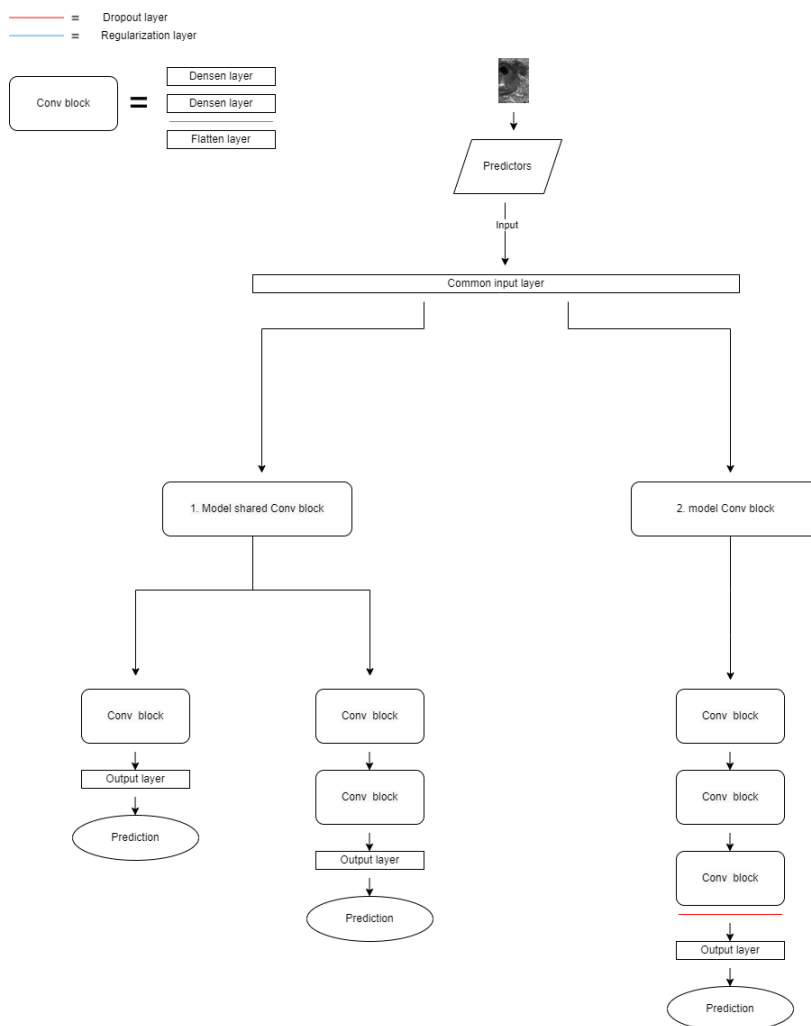


Figure 7.21: A representation of the final implemented network structure, which illustrates the branches as well as then output layers for prediction.

7.5.3 Implemented hyperparameters

To train the network a number of manually adjust hyperparameters has been implemented which was used to define the training. The implemented hyperparameters is presented in table 7.1

Hyperparameter	Implemented values model1/ model2
Batch size	15
Learning rate initial/final	Decaying 1e-2/1e-5
Epochs	Early stopping, patience=10
Optimizer	Adam
Number of layers model1/model2	8/10
Regulizer L1/L2	$L1 = 1 \cdot 10^{-6}$ / $L2 = 1 \cdot 10^{-8}$

Table 7.1: Table representing the final implemented hyperparameters for the prediction models

The hyperparameters was determined through an trial an error approach to obtain the lowest loss while retaining a stable training of the model. For the parameters a static batch size was used while the number of epochs and the learning rate was re-determined based on the network performance on the validation loss, throughout training. The number of epochs is determined using early stopping with a patience of 10, to prevent overfitting. The learning rate is a decaying learning rate meaning that it slowly decays in value within the predefined limitations. This is performed to avoid underfitting of the model by preventing unsuited adjustments in weights and thereby not reach the proper min of the loss. The optimizer implemented is the standard Adam optimizer, as this uses two gradient descend to obtain an efficient training and weight adjustment.

7.6 Validation

7.6.1 Predictors

For evaluation of the predictors is based on both a quantitative and qualitative assessment of the extracted predictors to determine if these are viable for the prediction of the lymph node motility and the displacement in scans acquired during treatment. This is performed through a qualitative and a quantitative assessment.

Qualitative assessment of predictors

For the qualitative assessment a graphical approach for representation of the different features is opted for to represented to output of the extracted features. These are used to assess if the pre-treatment are representative and related to the during scans to provide if these would be representative and if these where related to other in the same time and the future location. Furthermore this is used to evaluate if the presumed associations with the motility and displacements which was presented in section 4.4.1, is evident.

Quantitative assessment of predictors

The quantitative assessment of the predictors is performed to determine if there is an correlation between the different predictors and how the predictors is correlated to the future locations. Therefore a correlation analysis is used to determine if there is associations between the different predictors and the future location.

7.6.2 Prediction model

The implemented prediction network is based of regression and therefore prediction are evaluated as how much this deviates from the true value. [Hart, Stork, and Duda 2000; Zar 1999] A measure for this deviance between the predicted value and true value is error, which is be used as a metric to calculate the average deviation of the predicted from the true value. There is multiple evaluation metrics which can be used for regression problems, however most commonly three metrics are used for evaluating the performance, mean square error(MSE), Root mean square error(RMSE) and mean absolute error (MAE). To validate the system one of the most commonly used metrics MSE is used to calculate the difference between the predictions and the true value. The MSE is an error metric which measures the squared difference of the predicted value and the true value.

$$MSE = \frac{1}{n} \sum_{n=1}^n (y_i - \hat{y}_i)^2 \quad (7.3)$$

The calculation is based on the equation presented in 7.3, where n represent the number

of samples, y_i represents the predicted value and \hat{y}_i represents the true value. To determine if the correct COM is predicted each output of the model has to be evaluated. Therefore, the validation of the prediction model is performed by calculating the MSE for the x, y and z to determine the models error.

8 Results

8.1 Predictors

8.1.1 Qualitative assessment

The qualitative assessments of the extracted predictors is used to determine how the chosen predictors associates with the displacements and motilities which was presumed in section 7.2. Therefore, because these were presumed associations, they are evaluated in the following section to determine if these were true.

Volume

As a predictor the bladder, rectum volume was extracted given that these has previously been associated with the motility of the prostate. The volumes for the rectum and the bladder varied between patients and scans. The extracted volumes for each patient is presented in figure 8.3 and 8.2.

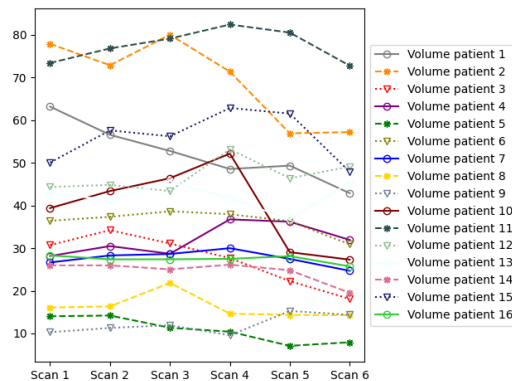


Figure 8.1: Illustration of the volume proportions for the tumor across scans for each of the patients with available annotations. Here scans 1, 2 and 3 is the pre-treatment scans and scan 4, 5 and 6 are acquired during treatment

For the bladder and rectum there were found to be inconsistencies of the volumes as these were varying and therefore the pre-treatment scan does not represent the volumes for the rectum or the bladder volume during treatment. There was found a larger bladder volume for multiple patients in the initial scan, while there was also found a larger rectum volume for multiple patients in the second scan, while the smallest volume for the rectum volume was found in the last scans for multiple patients.

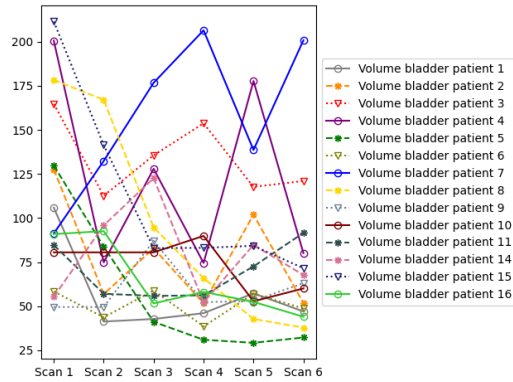


Figure 8.2: Illustration of the volume proportions for the Bladder across scans for each of the patients with available annotations of the bladder. Here scans 1, 2 and 3 is the pre-treatment scans and scan 4, 5 and 6 are acquired during treatment

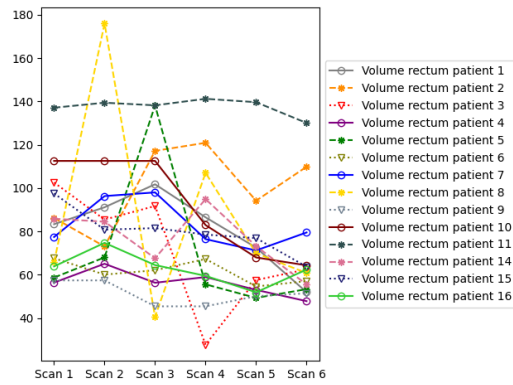
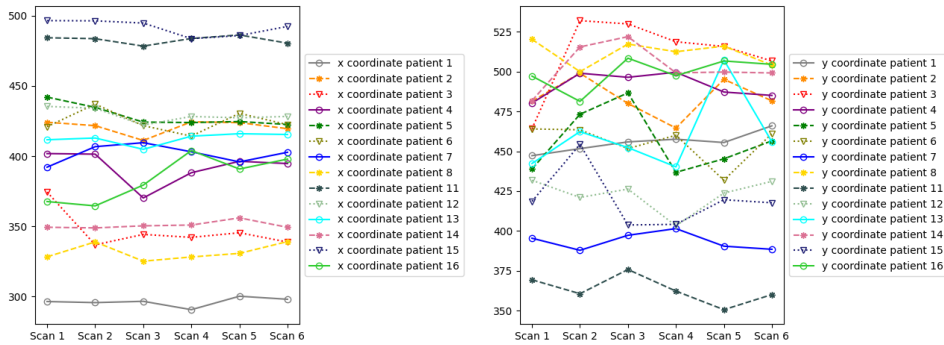


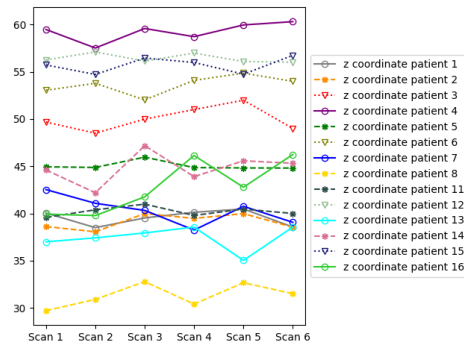
Figure 8.3: Illustration of the volume proportions for the Bladder across scans for each of the patients with available annotations of the rectum. Here scans 1, 2 and 3 is the pre-treatment scans and scan 4, 5 and 6 are acquired during treatment

Lymph nodes center of mass

It was assumed that the lymph node locations shift between because of the motility, and therefore these are assessed, to determine if there is a change in location. This is evaluated based on the COMs and the motilities extracted from different scans. The COMs is presented to determine if there is a change in the location and to see if these represents the area. The COMs of one lymph node for all patients illustrated in figure 8.1.1.



(a) x placement for one lymph node, where scans 1, 2 and 3 is the pre-treatment scans and scan 4, 5 and 6 are acquired during treatment (b) y placement for one lymph node, where scans 1, 2 and 3 is the pre-treatment scans and scan 4, 5 and 6 are acquired during treatment



(c) z placement for one lymph node, where scans 1, 2 and 3 is the pre-treatment scans and scan 4, 5 and 6 are acquired during treatment

Figure 8.4: A representation of the variation the x, y and z coordinate for center of mass for the same lymph nodes

The center of masses presented in figure 8.1.1 suggest that the displacement of the lymph nodes in superior-inferior (SI), appears to be systematic. This is evident in both the pre-treatment and during treatment scans. Similar patterns are not evident for the displacement in the ML and AP direction as these do not exhibit a repetitive pattern and

appears differently for each of the patients, throughout the pre-treatment and during treatment scans. It is however evident that there is changes in the COM location of the lymph nodes between scans, and these do exhibit similar area of location in the pre-treatment and during treatment scans.

Lymph nodes motility

Initially it was presented in section 4.4.1 that at motility of the lymph node in the pelvis was present, and the COM results suggest that there is a change in the location. As different associations was assumed to influence the motility, the lymph motility is evaluated to determine if this was true. The results for the quantified motility ranges between different scans for all patients is presented in figure 8.5, 8.6 and in figure 8.7.

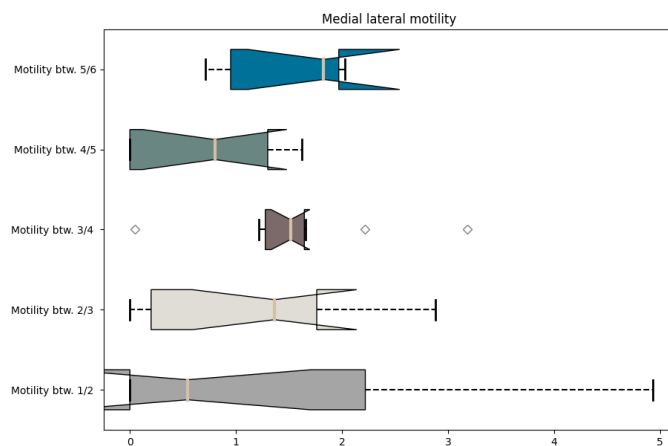


Figure 8.5: A representation of the estimated lymph node motility in the medial lateral direction. So 1/2 represents the motility estimated between the first and second scan

The presented plots show that the range of motility for the scans are largest between the first and second scan in the SI and ML direction. For the motility in the AP direction the obtained motility was representative of the motility in the remaining scans, however with there being a slightly larger range for motility obtained for scan 4/5, which could be contributed to increase in bladder volume for multiple patients. The motility in the AP direction co-exist with a significant change from large to smaller volume of the bladder for multiple patients between the first two scans. Thereby the size of the bladder might affect the motility of the lymph nodes. Similarly there was found to an higher average motility between the last two scans in the ML and SI direction which co-exists with a smaller rectum volume for multiple patients, which could indicate that the rectum volume likewise affects the motility of the lymph nodes. Additionally, there is found to generally to have slightly larger values for the motility between the first two scans and the last two scans in the SI and ML direction for multiple patients which is evident with

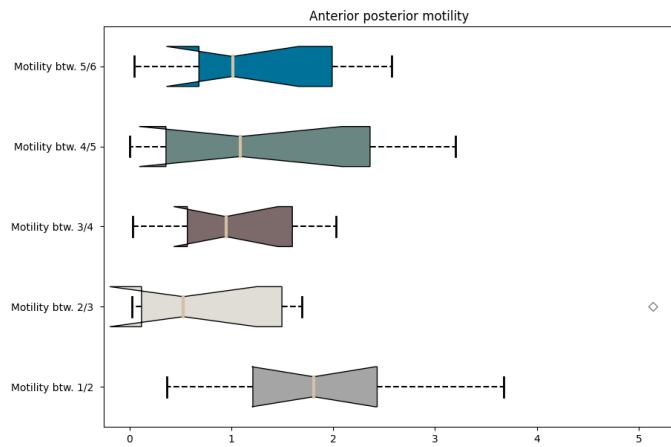


Figure 8.6: A representation of the estimated lymph node motility in the AP direction between scans. So 1/2 represents the motility estimated between the first and second scan

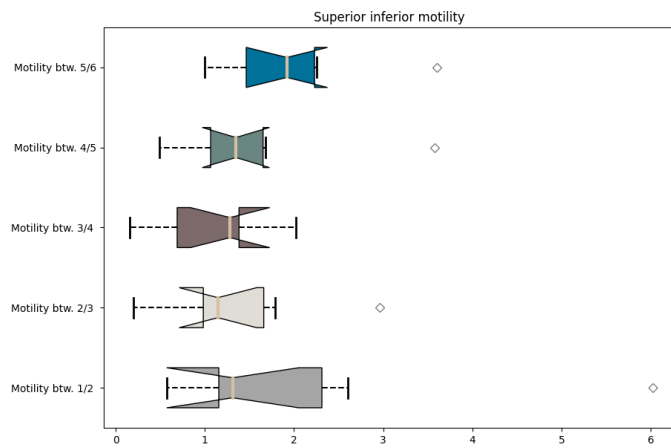


Figure 8.7: A representation of the estimated lymph node motility in the superior inferior between scans. So 1/2 represents the motility estimated between the first and second scan

smaller tumors volumes for multiple patients.

8.1.2 Quantitative assessment

In addition to the qualitative assessment a quantitative evaluation of the predictors is performed to determine if there is associations between the motility of lymph nodes, the COM and volumes as presumed in section 7.2. To obtain this quantitative assessment a correlation analysis is performed, which presents the correlation between the predictors, including the motility, and the future location of the lymph nodes. A figure representing the correlation between the predictors and the location is presented in figure 8.8.

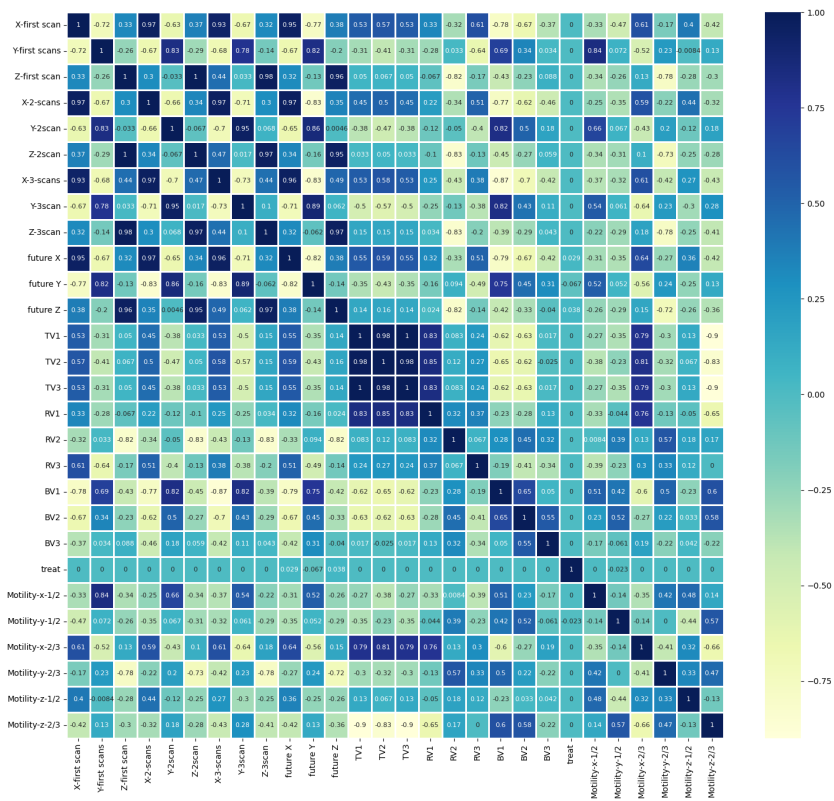


Figure 8.8: Illustration of the correlation analysis performed to determine if there is an association between the different predictors and the motility of the lymph nodes. Here the x-motility is the motility in the ML direction, y-motility is the motility in the AP direction and the z-motility is the motility in the SI direction

The correlation between the different predictors and the future location is presented in

figure 8.8. This suggest that there is association between the predictors and different parts of the coordinate, which represents the current and future location. The correlation analysis found a correlation for the x and y coordinate of the COM and the bladder volume which was indirectly found in the qualitative assessment as the motility in the AP and the bladder was associated. Furthermore, there was found to be a slight correlation between the motility in the ML direction, shown as Motility-x 2/3 was associated, and the rectum volume, which is compatible with the qualitative assessment which likewise found that the might be an association between the motility and the rectum volume. A high correlation between the motility in the SI direction represented as motility-z-2/3 and the tumor volume, which in the qualitative assessment was with the ML motility, presumed to be somewhat related to tumor volume or the disease progression.

Furthermore, there is found a high correlation in between the previous and future z coordinate, which could be associated with the identified pattern in described in qualitative assessment.

8.2 Data augmentation results

Data augmentation

Data augmentation was employed to increase the datasets size. This was obtained through training of stacked autoencoders, which produced new data with the same association between all the values, which is similar to the original dataset. The increase in the size of the dataset was achieved an illustration of the data samples and their distribution relative to to the true values is illustrated in figure 8.9.

There is a small deviance in the values, that has been augmented which is evident in the small blue edges which represent the true values on the figure 8.9. The precision of the augmented data samples varied where the new data samples for the volumes and the x and y coordinate generally distributed around the original values within the dataset , while values for the z-coordinates, texture features, and the motilities deviated significantly, was returned close to zero or to zero as illustrated for the motility in the AP and ML direction and therefore all the new augmented points are located on the same spot in the plots on the second row in figure 8.9.

8.3 Prediction model

Hyperparameters

For training of the network hyperparameters was used to determine the different aspects of training. The hyperparameters which was implemented in the network is presented in table 8.1. It was found that there was a deviation in the hyperparameters which produced a stabilized training for the two models, where the training of the final network models is shown to be stable with minor fluctuations in the training for all three coordinates.

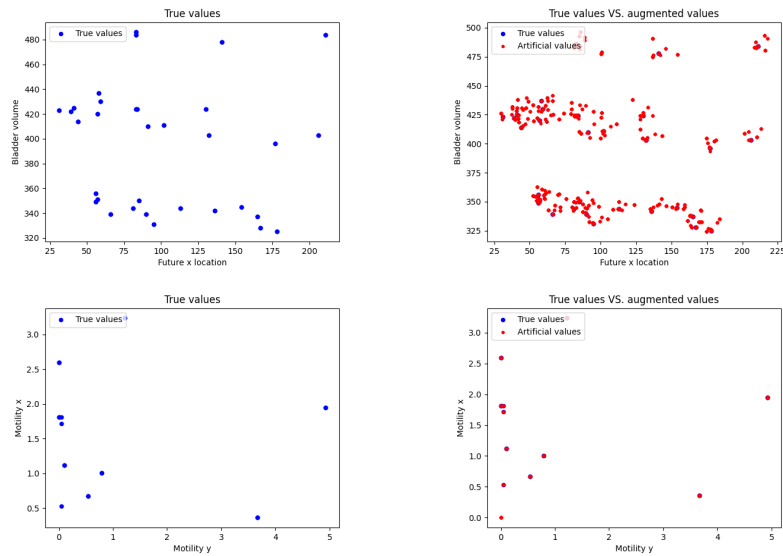


Figure 8.9: Illustration of the distribution of the bladder and tumor volume augmented where the red is augmented values and the blue with lies under some of these data points are the true values. Similarly the 3rd and 4th plots illustrate the distributions of the true values and augmented values for the motility in the ML and AP direction

Hyperparameter	Implemented values model1/ model2
Batch size	15
Learning rate initial/final	Decaying 1e-2/1e-5
Epochs	Early stopping, patience=10
Optimizer	Stochastic gradient descend
Number of layers model1/model2	8/10
Regulizer L1/L2	$L1 = 1 \cdot 10^{-6}$ / $L2 = 1 \cdot 10^{-8}$

Table 8.1: Table representing the final implemented hyperparameters for the prediction models

Prediction model

Different correlations between the predictors, as presented in figure 8.8, was found. Because of this different models was trained to determine which final input predictors produces models with the lowest loss. In particular the future location and motility was related to the organ volume and therefor models were trained, on dataset which excluded motility or volume, to evaluate which predictors produced a model with the lowest loss. The same model structure was used to train, these variations of the dataset, and the loss curves for these models are presented in figure 8.10.

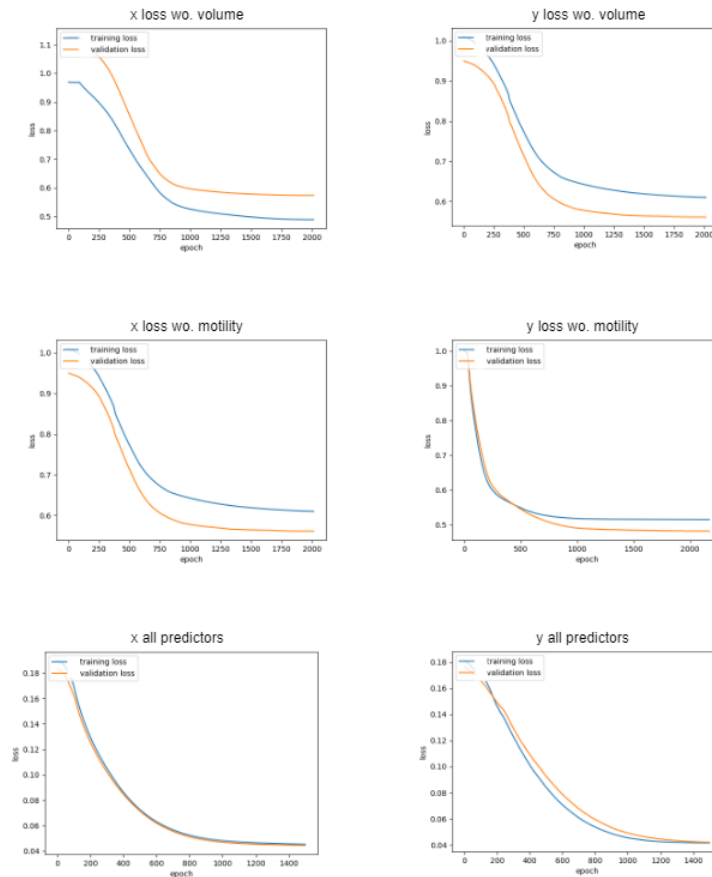


Figure 8.10: Illustration of the correlation analysis performed to determine if there is an association between the different predictors and the motility of the lymph nodes.

The loss curves in figure 8.10 suggest that the model could identify patterns and associations which is related with the future position. The final model which obtained the lowest loss was the model what was trained on the full dataset, that included all predictors and therefore the final validation is performed on this model.

Validation is performed using the test set, with the MSE as the validation metric, presented

in section 7.6. The validation MSEs for the final model is presented in table 8.2.

Output	MSE
Output layer X	0.009
Output layer Y	0.065
Output layer Z	0.057

Table 8.2: Output MSE prediction models

A high MSE is obtained for the currently trained model and thereby the positional predictions deviated from the true values of the lymph node locations which suggest that the current model, despite stable training, is incapable of generalization using the identified associations for predictions on new data.

9 Discussion

9.1 Results

The purpose of the project was to develop a model that could predict the future location of lymph nodes based predictors associated with the motility or the future location. To do this a pipeline consisting of extracting multiple predictors, data augmentation and a deep learning regression model to predict the next location, was proposed.

9.1.1 Identification and quantification of predictors

The assessment of the identified predictor both the quantitative and the qualitative revealed direct and indirect associations with the other predictors and the future location of the lymph nodes. Through the qualitative assessment it was revealed that an average larger motility in the ML and SI direction was present when there was a smaller rectum volume, while a larger bladder in the first scans with a smaller in the second scans for the pre-treatments scans co-existed with a larger range motility of the AP direction. The identified associations were likewise supported by the quantitative analysis which found a correlation of the bladder and rectum with the future locations and motility. These associations, in the quantitative and qualitative analysis, between the location and motility is compatible with findings in Roch, Zapatero, Castro, Büchser, et al. [2019](#) which likewise found there to be an association between the rectum and bladder size and location. Therefore, these results could be indicative that the assumption regarding the lymph nodes motility and volumes are true.

The qualitative assessment of the COM showed variation in the locations of the COMs which indicates that the COMs was somewhat representative of the area, in which the lymph nodes are located. However the z-coordinate revealed a particular pattern, as this occurred in a repetitive fluctuating pattern which is indirectly evident in the correlation analysis as there is a high correlation between the future and current locations. As this particular pattern is not evident in the volumes or motilities, this could indicate that the variance in this particular direction is affected by another predictor, other than the inverse correlated rectum volume, which has not been extracted such as respiration. Respiration exhibits a similar fluctuation pattern, and has previously been shown to have an impact on the motility of lymph nodes for cervical cancer. [Rai et al. [2016](#)] Therefore, an additional predictors which represents this should be included as a predictor to improve the performance of the model.

The estimated margins of the motility are inconsistent with the margins found in the study by Björelund et al. [2018](#). However, there is obtained an average larger margin in the AP direction when compared to SI, and ML directions which is similar to the study.

The estimated motility ranges is similar to the once found in Rai et al. 2016, where the margins, for pelvic lymph nodes, in the SI direction is within the same range to the once found in this study, while the margin for the AP and ML directions is slightly smaller. The motility is similar, but still deviates in the AP and ML direction, which could be attributed to the method which is used for quantification of this. The estimation of the motility was based on multiple registration of the images which each is prone to error that can accumulate with each alignment. This becomes evident in the final DVF, and therefore in the final translations, which are used as representations for the motility.

For the tumor volume the qualitative assessment, based on figure 8.1, showed a progression in tumor volume which increases or slightly fluctuates in the pre-treatment scans while a reduction occurs in the during treatment scans. These changes in the tumor volume provided an insight into the disease progression, where smaller volumes for the tumor was generally obtained in the first and last scans, this co-existed with an average larger motility between the first two scans and the last two scans in the ML and SI direction. This was likewise supported by the quantitative assessment was found a significant correlation between the tumor volume and the SI motility. These association might be attributed to less cancer tissue being present or less swelling of the damaged tissue in the first and final scans. This could indicate that there is a variation of the tissues, and therefore including different texture features contributed to quantifying the properties and describing how the tissue was altered throughout the disease-and treatment progression.

9.1.2 Data augmentation and prediction model

Data augmentation

Varying results was obtained regarding the output of the stacked autoencoder as the augmented values for most predictors was representative, such as the volumes and the COMs' while the motilities, textures and z coordinate was returned close to zero. The values close to zero could be associated with the range of values which are present in the dataset as an autoencoder is used to replicate the dataset by inducing small deviance from the original values. This might force the smaller values for these extracted parameters to return close to zero and induces noise and uncertainties into the model when training which could contribute to the high MSEs' for the final prediction model. Because of this another augmentation approach could be employed, to obtain additional data. This could be performed directly on the scans as the properties and relations between the stage of the pelvis and the lymph nodes motilities, is known. Therefore augmentation in a new manner which is based on this new knowledge could be developed, by generating scans which is based on these.

Hyperparameters

The implemented hyper parameters of the model was found through a trial and error approach, which might not be suitable for determining the hyperparameters as these influence the training of the model and therefore affects the final models performance. Therefore, a systematic approach to determining these values, such as grid search, should be employed for estimation of the the proper values for the current model which could improve the training and subsequent the generalization performance of the model.

Prediction model

Multiple prediction models was trained on the full dataset and on datasets which excluded certain predictors where the losses for the losses for the training is presented in figure 8.10. The training losses show that the model with the lowest loss was trained on a dataset which included all the predictors, and therefore despite the correlations between the predictors one predictor does not compensate for another, when training a prediction model. Therefore each of these predictors contributes to predicting the future location through improvements of the training and lowering of the loss. This further supported the choice of identified predictors in section 7.2, as the performance was reduced when predictors was removed. Despite this the final model still produced a high MSE during the validation and therefore there was a significant deviance between the predicted location of the lymph nodes and the true location of the lymph nodes. This deviance of the predicted values could be attributed to different parameters previously , or other parameters such as the included layer or the network structure.

The implemented network consist of three layer types, dense, regularization and dropout layers which was included as these are the common layers in prediction models, while also providing regulation of the weight and biases in the network. This might have affected the model performance as to much regularization could apply penalties to appropriately fitted weights and therefore increased the MSE. This could have been omitted by simplifying the model, but this might also reduce the model performance. Other model structures could be employed to obtain a model which has a lower error. Such a model could be designed as three separate models which each predict part of the coordinates which collectively estimates the COM location of the lymph nodes. A model design composed of three different models would be less reliant on balancing the losses from the different outputs of the model throughout training. Furthermore, the network parameters for this model structure would be fully be customized for the prediction of the individual coordinates. This would however not utilize of the co-dependencies and high correlation between the target coordinates shown location presented in the correlation analysis 8.8. Therefore, an alternative model type could be opted for.

Alternative model designs

Currently the model structure obtains a high MSE for the output of the model independently of predictors are presented as input, and therefore an alternative model could be opted for to estimating the future locations. An alternative could be to predict the future scans containing these locations which could be achieved, with a GAN network as in Mirzapour et al. 2019 and Dai et al. 2021. A GAN network could be utilized to predict the subsequent scan at a given time and then based on the newly predicted scans the locations would be extracted. For this approach to predicting the location, the multiple outputs which currently describe the location as well as balancing the losses, would be omitted, however this would require a significant amount of data to create this model.

Alternatively, this prediction could be defined as a probabilistic classification with many different classes where each voxel coordinate location is represented by a class. This approach could be used as there is limitations for the values which the future location of lymph nodes can have, and therefore a discrete approach such as classification could be used instead of an continuous prediction. The limitations for the values could be defined by different constraints such as the image dimensionalities which provides constraints to the possible values that can contain anatomical information while additional constrains, can be given by using the values for the motility range found in articles Rai et al. 2016 or Björelund et al. 2018 or by using the estimated calculated motility presented in section 8.1.1.

9.2 Limitations

There have been different limitations which is associated with the current model. These limitations are affiliated which different aspect of the model, the inputs, and the training of the final model. Limitations which has been identified to affect the model includes the available annotations combined with the method approach and the size of the dataset. Having a small dataset consisting of 16 patients, is a limited number of patients to provide a generalized picture of a patient population which therefore affects the models structure and the generalization of the model. In addition to this a varying number of annotations as presented in table 6.1. The model was build to predict the future location based on the scans acquired pre-treatment which generally consisted of 3 scans. However, there was not three scans available for all patients 9, and 10 was not included for training or validation of the model, furthermore a varying number of annotations was available and for patient 12 and 13 the annotations for the bladder and rectum was not available. As the patients lacked scans or annotations these were not included in the final dataset and therefore these was not included in the final dataset for the prediction model which consisted of 12 patients.

To omit the annotation limitation and thereby re-introduce patient 12 and 13 to the dataset, unsupervised segmentation approaches, such as region growing could be used to obtain the annotations. Based on the representation of the organs on the scans, these

methods could provide a viable representation of the organs. Unsupervised methods are however prone to having a lower accuracy of the outline, which would influence the extracted volumes and this could further negatively impact the MSE of the model, if the segmentations are not reliable.

Segmentation reliability of the lymph node annotations is also a limitation which could influence the model performance. The COMs was based on the segmentations provided by a deep learning model developed prior to the project which has a slight error and thereby did not represent the full lymph node outline, this could have provided inaccuracies which would be evident in the calculated COMs. This would influence the training of the model and subsequent the output of the model, and therefore the accuracy of the segmentation model provided a limitation to the model.

9.3 Future perspectives

The aspect of predicting the future location based on previous scans and predictors can be applied for other types of cancer or to other physiological phenomena. This methods could be used with multiple other types of cancer where radiotherapy treatment is applied. It be utilized to predict the future location of the lymph nodes and maybe tumor to decrease the area of application, to refine the volumes, and reduce the amount of damaged healthy tissue. This could however require to identify other predictors which is specific to this type of cancer, as this would be area specific. An area such as in the lung, could introduce this concept where the respiratory phase could be used as a predictor.

Another aspects were it could be beneficial to use such a system when looking a blood flows. This could be used to determine whether blood flow is turbulent or not, using the previous location and viscosity as a predictors. A specific target could be represented by a marker which in blood could be an air bubble as this would be evident in scans. Significant deviance in the specific target value and the predicted value could be indicative of a turbulent flow of the blood.

Although there could be different applications of the specific methodology and altered versions of this the current model need further development and alterations for it to be applicable in clinical practice is needed.

This page intentionally left blank.

10 Conclusion

The project aim was to develop a model which could predict the location of the lymph nodes in scans acquired during treatment. An approach for this was presented in chapter 7.1 which consisted on extracting different predictors and which was used as input to a deep learning regression model, which produced an output prediction of the lymph node location. For the presumed assumptions there was found to be associations for the rectum and bladder volumes and the motility of the lymph nodes in different directions. This, therefore, indicates that the assumptions made regarding the lymph node motility was true. However other predictors exhibited pattern which was not similar to the motility and therefore additional predictors associated with this should be identified. Based on the extracted loss plots these suggest that the presented model structure was able to identify association within the predictors and therefore the features to determine the future position. However, the validation suggests a large error and thereby the models generalization performance is low, which can be attributed to a small dataset, the extracted predictors, or the model structure. Therefore another model design should be employed to improve the generalization, while acquiring additional data, identifying new predictors and include new predictors which could contribute to obtain a model with a better generalization performance.

This page intentionally left blank.

11 Portfolio

This portfolio is regarding the project management throughout the 10th semester on biomedical engineering and informatics. The following portfolio describes the the process for the work,including the motivation for the project and the opted approach for the project work, as well as the method for time management throughout the semester. Lastly the the project was performed with external collaboration, which will likewise be described.

11.1 Motivation

Throughout my masters degree the focus has been to explore current and develop new methods for signal and image processing and analysis. This provided different competencies and insight into approaches for analyzing and processing images, therefore the motivation for this project has been to develop methods which could contribute to improve the current treatment rectal cancer using these competencies. It through literature it was identified that there is currently few assessments of different aspects which affects the lymph nodes motility, and no model for predicting the future location of the lymph nodes. This absence of knowledge regarding the associations with the pelvis lymph nodes and the lack of method for determining the future location provided a constraint for decreasing the area for application of radiotherapy, as the location during treatment is unknown. Therefore to provide a contribution to the currently unresolved problem, I tried to contribute using existing competencies and develop new competencies within image processing and analysis, to identify the pelvis' organs associations with the lymph nodes location and motility and develop a model which could predict the future location so the area of application could be decreased. Thereby contributing to investigating this area, remove this limitation and improve the treatment of rectal cancer.

11.2 Work approach

The process for the work throughout the development and execution of the project was an iterative. This iterative approach was employed for the background, design and the development of the model. The approach was employed as the design and implementation of the final model was depended on the output of the previous steps in the pipeline including the presumed assumptions as well as the size of the dataset. Furthermore this process was iterative as the design of the prediction model was found through literature, while also being impacted by other factors which influence the structure and performance. Therefore the literature, data and predictors were revisited on multiple occasions to

obtain a final model structure. The re-visiting to the literature to determine the pipeline allowed for looking into different fields to gain knowledge of how to approach some of limitations and models, as no previously models for location prediction has been identified, and thereby there was no previous model as an starting point. This provided inputs from different aspects and fields to generate, the final pipeline.

This was however goal oriented as it is very target specific , which might have induced a slight bias into the pipeline design and thereby into the obtained results.

11.3 Time management

The work progress was in an iterative manner and to manage this and to produce a final product a time table was utilized. Time management was performed using a time schedule which was derived in the initial stages of the project and the iterated throughout the project duration to compensate for the addition to new tasks or to adjust for unforeseen changes. This time schedule was developed is presented in the following section.

11.3.1 Time schedule

To structure the project and time though-out the semester and example is this is presented in figure 11.1

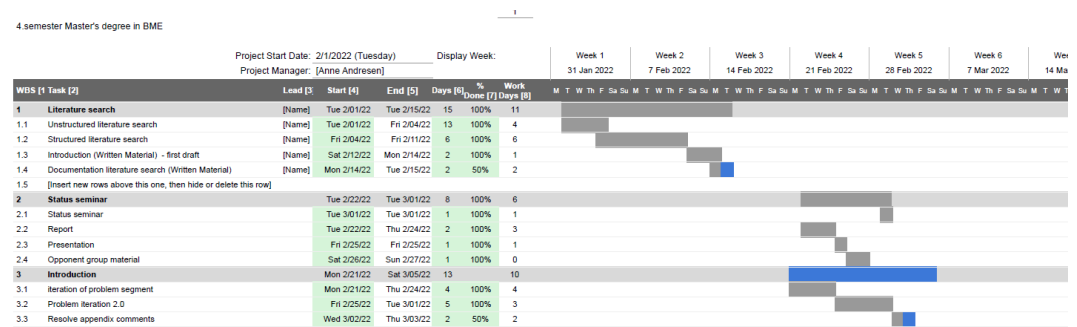


Figure 11.1: A representation of the constructed time table which was used for time management

The construction of the time table is based on initially on defining the task which in the presented figure 11.1 is shown to the left. These consist of all the different task which has to be written or a task which has to be performed is included to delineate a overview of the different aspects which the project consists of. These task are grouped into different pools according to larger segments of the project rapport such as background, method or results, which then provides an overview of completion of different segments of the rapport.

Following the definition of the tasks a timeline for the different tasks is established through back casting from the deadline. This timeline is presented in a multitude of ways to provide additional information regarding when the task is performed, how long it takes, the time which has already been used on the task and visual representation of the duration of the individual task over the entirety of the semester. The different time definitions are represented in the columns which are placed subsequent to the column defining the individual task. Thereby the time which is provided for each task is placed subsequent to the specific task. The task duration is visualized the row of the specified task across a time series which represents the semester. The length of the row is determined based on the start and end date which then colors the rows of that time span. The coloration of these are in two colors, one which represents active task and tasks which have not been completed, blue and the other representing when completed, gray. This visualization is likewise presentment in figure 11.1

11.4 Supervisor

Supervisor meetings were held consistently throughout the 10th semester to provide feedback on written material, inputs regarding the projects background and the development and design of the solutions. This furthered the project through out the semester by giving inputs and question which allowed for reflection of the current methods and contents of the project. Furthermore, supervisor likewise provided drop-in supervision either in person or through email where quick questions or inputs to the project which did not require an entire meetings, where discussed or answered.

11.5 External collaborations

The semester was performed with external collaboration from the Aalborg university hospital which provided data, as well as insight into different aspect of the project. As these had different backgrounds which provided insights and knowledge from different fields.

The external collaborators provided help in a multitude of ways such as providing articles which contributed to different aspects of the project in the background, methods and discussion. Furthermore the external collaborators provided insights into how to interpret the outputs of steps in the project and suggested different aspect could influence these. Thereby different aspects of the background and results were provided which contributed to the development as well as the interpretation and discussion of the results of the project.

This page intentionally left blank.

Bibliography

- Adams, Robert A and Christopher Essex (1999). *Calculus: a complete course*. Vol. 4. Addison-Wesley Boston.
- Akino, Yuichi et al. (2013). “Estimation of rectal dose using daily megavoltage cone-beam computed tomography and deformable image registration”. In: *International Journal of Radiation Oncology* Biology* Physics* 87.3, pp. 602–608.
- Bahadoer, Renu R et al. (2022). “Watch and wait after a clinical complete response in rectal cancer patients younger than 50 years”. In: *British Journal of Surgery* 109.1, pp. 114–120.
- Bairstow, Rhianna et al. (2020). “Evaluation of seminal vesicle volume variability in patients receiving radiotherapy to the prostate”. In: *Journal of Radiotherapy in Practice* 19.1, pp. 20–24.
- Bell, Linda J et al. (2021). “Intra-fraction displacement of the prostate bed during post-prostatectomy radiotherapy”. In: *Radiation Oncology* 16.1, pp. 1–11.
- Björelund, Ulrika et al. (2018). “Inter-fraction movements of the prostate and pelvic lymph nodes during IGRT”. In: *Journal of radiation oncology* 7.4, pp. 357–366.
- Brahme, Anders (2014). *Comprehensive biomedical physics*. Newnes.
- Burnet, Neil G et al. (2004). “Defining the tumour and target volumes for radiotherapy”. In: *Cancer Imaging* 4.2, p. 153.
- Chen, Haibin et al. (2018). “Internal motion estimation by internal-external motion modeling for lung cancer radiotherapy”. In: *Scientific reports* 8.1, pp. 1–14.
- D’Amata, Gabriele et al. (2021). “The “Watch and wait” approach following chemoradiotherapy for rectal cancer”. In:
- Dai, Xianjin et al. (2021). “Deep learning-based motion tracking using ultrasound images”. In: *Medical Physics* 48.12, pp. 7747–7756.
- Dizdarevic, Edina et al. (2020). “Long-term patient-reported outcomes after high-dose chemoradiation therapy for nonsurgical management of distal rectal cancer”. In: *International Journal of Radiation Oncology* Biology* Physics* 106.3, pp. 556–563.
- Dossa, Fahima et al. (2017). “A watch-and-wait approach for locally advanced rectal cancer after a clinical complete response following neoadjuvant chemoradiation: a systematic review and meta-analysis”. In: *The lancet Gastroenterology & hepatology* 2.7, pp. 501–513.
- Gonzalez, Rafael C, Richard E Woods, and Barry R Masters (2009). *Digital image processing*.
- Hart, Peter E, David G Stork, and Richard O Duda (2000). *Pattern classification*. Wiley Hoboken.
- Hearn, N et al. (2021). “Neoadjuvant radiotherapy dose escalation in locally advanced rectal cancer: a systematic review and meta-analysis of modern treatment approaches and outcomes”. In: *Clinical Oncology* 33.1, e1–e14.

- Hill, Derek LG et al. (2001). "Medical image registration". In: *Physics in medicine & biology* 46.3, R1.
- How does chemotherapy work? [updated 22. august 2019]* (2007). eng. Institute for Quality and Efficiency in Health Care. ISBN: NBK279427.
- Keras (2022). Conv2DTranspose layer. Accessed 20/05/2022. URL: https://keras.io/api/layers/convolution_layers/convolution2d_transpose/ (visited on 05/20/2022).
- Keras (2022). Conv2DTranspose layer. Accessed 20/05/2022. URL: https://keras.io/api/layers/convolution_layers/convolution2d_transpose/ (visited on 05/20/2022).
- Keras (2022). Conv2DTranspose layer. Accessed 20/05/2022. URL: https://keras.io/api/layers/convolution_layers/convolution2d_transpose/ (visited on 05/20/2022).
- Kershaw, Lucy et al. (2018). "Image guided radiation therapy strategies for pelvic lymph node irradiation in high-risk prostate cancer: motion and margins". In: *International Journal of Radiation Oncology* Biology* Physics* 100.1, pp. 68–77.
- Kim, Hyun et al. (2021). "Nonoperative rectal cancer management with short-course radiation followed by chemotherapy: a nonrandomized control trial". In: *Clinical colorectal cancer* 20.3, e185–e193.
- Krishnatry, Rahul et al. (2021). "Indigenous groin board immobilization reduces planning target volume margins in groin radiotherapy". In: *Journal of Medical Physics* 46.2, p. 88.
- Lawes, R et al. (2021). "Retrospective audit of inter-fraction motion for pelvic node radiotherapy in prostate cancer patients". In: *Radiography* 27.2, pp. 266–271.
- Lefébure, Martin and Laurent D Cohen (2001). "Image registration, optical flow and local rigidity". In: *Journal of Mathematical Imaging and Vision* 14.2, pp. 131–147.
- Löfstedt, Tommy et al. (2019). "Gray-level invariant Haralick texture features". In: *PloS one* 14.2, e0212110.
- Lorimer, Patrick D et al. (2017). "Pathologic complete response rates after neoadjuvant treatment in rectal cancer: an analysis of the national cancer database". In: *Annals of surgical oncology* 24.8, pp. 2095–2103.
- Maani, Elizabeth V and Christopher V Maani (2019). "Radiation Therapy". In:
- Mah, Dennis et al. (2002). "Measurement of intrafractional prostate motion using magnetic resonance imaging". In: *International Journal of Radiation Oncology* Biology* Physics* 54.2, pp. 568–575.
- Mahadevan, Vishy (2014). "Anatomy of the rectum and anal canal". In: *Surgery (Oxford)* 32.4, pp. 159–164.
- Marnouche, EA et al. (2021). "Evaluation of margins in pelvic lymph nodes and prostate radiotherapy and the impact of bladder and rectum on prostate position". In: *Cancer/Radiothérapie* 25.2, pp. 161–168.
- Mirzapour, Seyed Ali et al. (2019). "Intra-fraction motion prediction in MRI-guided radiation therapy using Markov processes". In: *Physics in Medicine & Biology* 64.19, p. 195006.

- Miyamoto, Eizan and Thomas Merryman (2005). "Fast calculation of Haralick texture features". In: *Human computer interaction institute, Carnegie Mellon University, Pittsburgh, USA. Japanese restaurant office*.
- Al-Najami, Issam et al. (2021). "Rectal cancer: Watch-and-wait and continuing the rectal-preserving strategy with local excision for incomplete response or limited regrowth". In: *Surgical Oncology* 37, p. 101574.
- Oates, R et al. (2017). "Real-time image-guided adaptive-predictive prostate radiotherapy using rectal diameter as a predictor of motion". In: *Clinical Oncology* 29.3, pp. 180–187.
- Pang, Xiaolin et al. (2021). "Management of Clinically Involved Lateral Lymph Node Metastasis in Locally Advanced Rectal Cancer: A Radiation Dose Escalation Study". In: *Frontiers in oncology*, p. 2723.
- Papaccio, Federica et al. (2020). "Neoadjuvant Chemotherapy in Locally Advanced Rectal Cancer". In: *Cancers* 12.12, p. 3611.
- Pilskog, Sara et al. (2020). "Plan selection in proton therapy of locally advanced prostate cancer with simultaneous treatment of multiple targets". In: *International Journal of Radiation Oncology* Biology* Physics* 106.3, pp. 630–638.
- Pos, Floris J et al. (2003). "Influence of bladder and rectal volume on spatial variability of a bladder tumor during radical radiotherapy". In: *International Journal of Radiation Oncology* Biology* Physics* 55.3, pp. 835–841.
- Poulsen, Laurids Østergaard and et. al (2021). *Adjuverende kemoterapi ved rektumcancer*. <https://dccg.dk/retningslinjer/kolorektal-cancer/#1502740758880-76f8c030-6fe2>. Online; besøgt d. 8-9-2021 år.
- Qiu, Peng et al. (2007). "Inferential modeling and predictive feedback control in real-time motion compensation using the treatment couch during radiotherapy". In: *Physics in Medicine & Biology* 52.19, p. 5831.
- Rafaelsen, Søren R et al. (2013). "Ultrasound elastography in patients with rectal cancer treated with chemoradiation". In: *European journal of radiology* 82.6, pp. 913–917.
- Rai, B et al. (2016). "Margins Around the Involved Pelvic Lymph Nodes for Planning Simultaneous Integrated Boost in Patients With Cervical Cancer Undergoing Pelvic Intensity Modulated Radiation Therapy". In: *International Journal of Radiation Oncology, Biology, Physics* 96.2, E316.
- Ramsundar, Bharath and Reza Bosagh Zadeh (2018). *TensorFlow for deep learning: from linear regression to reinforcement learning*. " O'Reilly Media, Inc."
- Recio-Boiles, Alejandro et al. (2018). "Rectal Cancer". In:
- Rega, Daniela et al. (2021). "Watch and Wait Approach for Rectal Cancer Following Neoadjuvant Treatment: The Experience of a High Volume Cancer Center". In: *Diagnostics* 11.8, p. 1507.
- Roch, Maria, A Zapatero, P Castro, D Büchser, et al. (2019). "Impact of rectum and bladder anatomy in intrafractional prostate motion during hypofractionated radiation therapy". In: *Clinical and Translational Oncology* 21.5, pp. 607–614.
- Roch, Maria, A Zapatero, P Castro, D Hernández, et al. (2021). "Dosimetric impact of rectum and bladder anatomy and intrafractional prostate motion on hypofractionated prostate radiation therapy". In: *Clinical and Translational Oncology* 23.11, pp. 2293–2301.

- Serway, Raymond A and John W Jewett (2018). *Physics for scientists and engineers*. Cengage learning.
- Shiao, Jay C, Kareem Riadh Fakhoury, and Jeffrey Olsen (2020). "Total Neoadjuvant Therapy for Rectal Cancer: Current Status and Future Directions". In: *Current Colorectal Cancer Reports*, pp. 1–10.
- Siegel, Rebecca, Carol DeSantis, and Ahmedin Jemal (2014). "Colorectal cancer statistics, 2014". In: *CA: a cancer journal for clinicians* 64.2, pp. 104–117.
- Siegel, Rebecca L et al. (2020). "Colorectal cancer statistics, 2020". In: *CA: a cancer journal for clinicians* 70.3, pp. 145–164.
- Spindler, Karen-Lise Garm et.al (2021). *DCCG'S NATIONALE RETNINGSLINIER FOR DIAGNOSTIK OG BEHANDLING AF KOLOREKTAL CANCER*. <https://dccg.dk/retningslinjer/kolorektal-cancer/#1502740758880-76f8c030-6fe2>. Online; besøgt d. 8-9-2021 år.
- Su, Zhong et al. (2019). "PTV margin analysis for prostate patients treated with initial pelvic nodal IMRT and prostate proton boost". In: *Physics in Medicine & Biology* 64.4, 04NT04.
- Tensorflow (2021). Conv2DReg layer. Accessed 20/05/2021. URL: https://www.tensorflow.org/api_docs/python/tf/keras/regularizers/L2.
- Van Liew, S et al. (2007). "MO-E-M100F-06: Intra-Fraction and Inter-Fraction Real-Time Tumor Motion Prediction Using Multiple External Surrogates". In: *Medical Physics* 34.6Part16, pp. 2529–2529.
- Velema, LA et al. (2012). "Oc-0463 nodal Ctv deformation cannot be neglected in highly conformal radiotherapy of cervical cancer patients". In: *Radiotherapy and Oncology* 103, S185–S186.
- Wang, Yalin, Chenliang Liu, and Xiaofeng Yuan (2020). "Stacked locality preserving autoencoder for feature extraction and its application for industrial process data modeling". In: *Chemometrics and Intelligent Laboratory Systems* 203, p. 104086.
- Wu, James S (2007). "Rectal cancer staging". In: *Clinics in colon and rectal surgery* 20.03, pp. 148–157.
- Zar, Jerrold H (1999). *Biostatistical analysis*. Pearson Education India.
- Zhang, Xuan et al. (2022). "Efficacy and safety of the "watch-and-wait" approach for rectal cancer with clinical complete response after neoadjuvant chemoradiotherapy: a meta-analysis". In: *Surgical Endoscopy*, pp. 1–12.

A Literature search

The databases which are utilized as tools for obtaining the literature are *PHYSICAL REVIEW JOURNALS* Published by the American Physical Society, *PubMed*, *Embase* and *IOP SCIENCE*. These are utilized for accessing material as these allow for addressing medical as well as the physics aspects of the problem. The final literature search was performed the 27th february 2022, using a search query consisting of keywords combined using the operators **AND**, **OR** and **NOT**. Keywords were identified through an initial unstructured literature search which provided the and based on the a query string was constructed. This was searched in the four previously mentioned databases. The keyword included in the search queries is presented in table A.1, for the motility methods and A.2, for the prediction and quantification. These table represent the searches performed for the methods presented in section 4.4.1 and 4.4.2.

AND				
OR	Motion	Pelvis	organ	Quantification
	Movement	Rectum	lymph node	Estimation
	Motility			

Table A.1

AND			
OR	Intra fraction motion	Prediction	Model
	Intra fraction movement	Predict	Models
	Intrafraction motility		Association
			Regression

Table A.2

Once the searched for the respective areas there where for motility estimation found 157 number of articles and the prediction models found 67 number of articles. Subsequent to identification of the article these were sorted according to pre-defined requirements to the articles which excluded article which were not relevant for the study. The process and number of articles from the literature search is presented in the following prisma charts in figure A.1 and in figure A.2.

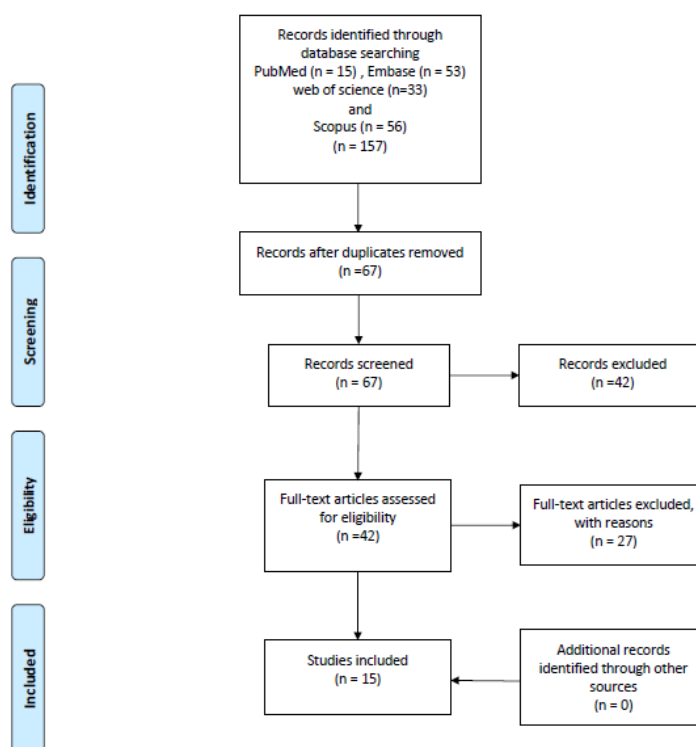


Figure A.1: Illustration of the prisma charts which describes the approach for obtaining literature which contains the currently developed methods for estimation of motility in the pelvis area with a focus regarding lymph nodes presented in section 4.4.1

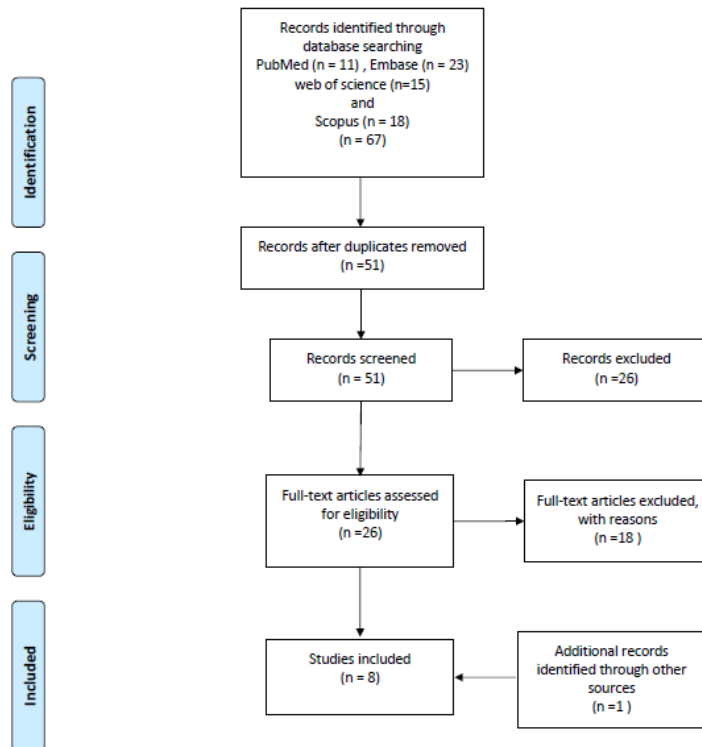


Figure A.2: Illustration of the prisma charts which describes the approach for obtaining the currently proposed methods for prediction in section 4.4.2